Supplementary Information for

Differences in signalling by directly and indirectly binding ligands in bacterial chemotaxis

Silke Neumann, Clinton H. Hansen, Ned S. Wingreen and Victor Sourjik

Supplementary methods

Receptor quantification

Cells for western blot analysis were grown as for FRET experiments (see Material and Methods). For the determination of antibody specificity, 1 ml of VS275 cell culture expressing receptor-YFP fusions from pTrc plasmids listed in Table SII was harvested for each Western blot or FACS analysis by centrifugation for 2 min at 13,300 rpm in a table-top centrifuge. For the Western blot analysis, the bulk of medium was removed after a first centrifugation. However, as a *cheR cheB* cell pellet disperses after a short period of time, the residual medium was removed after centrifugation for another minute and the pellet was immediately frozen in liquid nitrogen. For relative YFP quantification with a FACScan (Becton Dickinson), fluorescent cells as well as non-fluorescent control cells were washed twice with tethering buffer and diluted 1:20. To determine the antibody specificity, pellets of cells carrying the analyzed receptor-YFP fusions were adjusted to the same FACS value, e.g. YFP concentration, by resuspension in an appropriate volume of 1x Laemmli buffer. Samples were boiled 2x for 5 min at 95°C with intermediate vortexing. A dilution series of each sample was applied on a 10% SDS polyacrylamide gel. After separation by electrophoresis, proteins were transferred to a 0.2 µm pore size Hybond ECL nitrocellulose membrane using a tank blot device (BioRad) for 1h at 100 V in transfer buffer (25 mM Tris, 96 mM glycine, 0.02% SDS, 10% methanol). The membrane was blocked for 30 min in 10% instant non-fat dry milk/ TBST [150mM NaCl, 20mM Tris-HCl (pH7.5), 0.2% Tween20] on a rocking

platform and incubated overnight with polyclonal primary rabbit αTrg (kindly provided by G. Hazelbauer) or αTar antibody. Membranes were washed five times (5 min each) with TBST, incubated for 30 min at room temperature with 1:10,000 dilution of secondary antibody conjugated to IRDye® 800 (Rockland) and washed again as described above. Membranes were scanned with an Odyssey® Imager (LI-COR) and protein bands were quantified using ImageJ software (http://rsbweb.nih.gov/ij). To control the consistency of YFP concentration in the samples and to rule out degradation of the receptor YFP-fusions, Western blots were performed with αGFP Living Colors Av Monoclonal Antibody (JL-8; Clontech) and IRDye® 700 conjugated secondary antibody (Rockland).

In receptor titration experiments, Tar and Trg were expressed from pVS123 and pSN43, respectively, in strain SN23 at the same inductions as used for FRET experiments (see *Materials and methods*) and analyzed with αTar antibody. To take account for natively expressed Trg, its level was determined in SN23 carrying the empty pKG110 vector and subtracted as background from other Trg titration points.

For determination of changes in receptor expression in dependence of optical density (Fig. S6) 1 ml culture was prepared for immunoblot as described above. To adjust samples to the same protein concentration, a culture with OD_{600} = 0.45 was resuspended in 250 µl of 1x Laemmli buffer, and the Laemmli buffer volume for other samples was chosen according to their initial OD_{600}.

Receptor methylation profiles

To study methylation of Tar upon stimulation with different ligands (Fig. S9), cells were stimulated with indicated attractants while shaking on a rotary platform for proper mixing and aeration, and adaptation was allowed to proceed for 10 min. For the metabolizable substrates maltose and aspartate, 1 mM was added again every minute resulting in a maximum final concentration of 10 mM. The last stimulus was added right before 1.5 ml of cells were taken

out and pelleted for 1 min at 13,300 rpm in a table-top centrifuge. The medium was removed and the cell pellet was immediately frozen in liquid nitrogen to yield a snapshot of receptor methylation. 250 µl 1x Laemmli preheated at 95°C was added to frozen cell-pellets and samples were further prepared as described above. Receptors were separated on an 8% SDS polyacrylamide gel at 250 V overnight. Immunoblot with αTar antibody was performed as described above. Positions of different Tar methylation states were estimated from receptor bands of *cheR* strain VS126*, cheR cheB* strain VS275 *and cheB* strain VS124 applied to the same gel.

Data evaluation procedure

The value of FRET between CheZ-CFP and CheY-YFP, which reflects the concentration of CheY-P/CheZ complex and thus provides the measure of kinase activity, was calculated from changes in the ratio of yellow to cyan fluorescence signals as described by Sourjik et al, 2007 *Methods in Enzymology* 423: 363-391, using the following equation:

$$FRET = \frac{\Delta R_{\max} - \Delta R}{\frac{\Delta Y}{\Delta C} + R_0 + \Delta R_{\max} - \Delta R}$$

Here ΔR corresponds to the amplitude of the response (before onset of adaptation) and was calculated for each stimulus concentration as the difference of the ratios R_1 - R_2, where R_1 is the YFP/CFP ratio at steady state in the buffer and R_2 is the YFP/CFP ratio after stimulation. ΔR_{max} is the change in the YFP/CFP ratio after a saturating stimulus of attractant and R_0 is the ratio in the absence of energy transfer stimulated by addition of a saturating amount of attractant. $\Delta Y/\Delta C$ is the constant ratio of YFP decrease to CFP increase after a stimulus, which was determined to be 2.3 for the used microscope setup. Calculated FRET values were normalized to the steady state FRET in absence of attractant. For dose response curves FRET

values were plotted for a sequence of increasing attractant concentrations and fitted to a multisite Hill model. Note that because $\Delta Y/\Delta C + R_0 \approx 4 >> \Delta R_{max} \approx 0.1$, relative FRET value could be well approximated by $(\Delta R_{max} - \Delta R)/\Delta R_{max}$.

In dynamic range experiments, each 3-fold raised attractant concentration was added after cells have adapted to the prestimulus ambient ligand concentration. Here, the response amplitude was determined as the difference of the ratios R_A-R_2, where R_A is the YFP/CFP ratio for the adapted state at the prestimulus ambient concentration. The values were normalized to the value of ΔR_{max}, which reflects the steady state FRET in absence of attractant.

In adaptation precision experiments, cells were stimulated and allowed to adapt until no obvious changes occurred, maximally for 45 min. Adaptation precision A_p was determined using the following equation

$$A_p = \frac{1 - (\Delta R_{\max} - R_A)}{\Delta R_{\max}},$$

where $\Delta R_{max} - R_A$ describes adaptation imprecision, e.g. the difference between the steady state kinase activity and adapted kinase activity in presence of ambient ligand.

Supplementary figure legends

Figure S1. FRET-based kinase activity assay. Fluorescence resonance energy transfer (FRET) occurs upon complex formation between the phosphatase CheZ fused to cyan fluorescent protein (CFP) and the phosphorylated response regulator CheY fused to yellow fluorescent protein (YFP; A, right). FRET is monitored by directly exciting CFP and measuring CFP and YFP fluorescence in corresponding emission channels, whereby higher ratio of YFP / CFP emission is indicative of higher FRET (A, left, and B). The CheY-P level is modulated by the kinase CheA (not shown) upstream of CheY. In adapted state, CheA has an intermediate activity that can be observed as basal FRET (A). Addition of attractant, 18 µM and 180 µM maltose in (A), leads to a rapid reduction in the kinase activity and hence in the CheY-P level. It is followed by CheR-mediated receptor methylation, resulting in a gradual increase of activity and the YFP / CFP ratio back to the basal level (dashed line in A). Removal of attractant leads to an overshoot of the kinase activity, upon which it is rapidly reset to the basal level via CheB-mediated receptor demethylation. A steady slow increase of the adapted YFP / CFP ratio during the course of the measurement (dashed line in A) is due to faster bleaching of the directly excited donor molecule CFP than of the indirectly excited acceptor molecule YFP (B). Signals in (A) and (B) were each normalized to the initial value at t = 0 s for better comparability.

Figure S2. Comparison of dose responses at different pump rates. Examples of ligand-specific shifts in the dose-response curves for aspartate (A), serine (B) and ribose (C) acquired at the maximal flow rate of 2500 µl/min (closed symbols) and at the routinely used flow rate of 500 µl/min (open symbols). Error bars indicate standard errors.

Figure S3. Dynamic range of the response for directly and indirectly binding ligands. (A) Example of a part of the dynamic range FRET measurement for serine, starting with a

saturating stimulus of 30 μM Ser. Ligand concentrations were raised in 3-fold steps (black arrows) and cells were allowed to adapt to each current ambient concentration. YFP / CFP ratio corresponding to zero kinase activity at the beginning and the end of the measurement was determined using a saturating stimulus of 100 μM MeAsp (grey arrows). With increasing ligand concentration, adaptation precision to serine gradually decreases, as visible by a large offset between the adapted state in presence of serine and the unstimulated activity (interpolated from the measurements of adapted activity in buffer at the beginning and at the end of the measurement, shown by the dashed line). This failure of adaptation reduces response amplitude at high ligand concentrations. (B) Dynamic range measurement for galactose, exemplary for all indirect ligands. Cells start responding at the detection threshold, and the response reaches its maximum at the peak of the dynamic range in Fig. 1C. Dashed line indicates adapted kinase activity in buffer, determined as in (A) whereby second measurement in the buffer at the end of the experiment is not shown. Gradual steady drift of the base line during measurements in (A) and (B) is due to the change in the ratio of YFP to CFP over time due to faster bleaching of CFP (see Fig. S1), and is not related to changes in the pathway activity. (C-F) Cartoons illustrating responses to directly and indirectly binding ligands at low and high concentrations. For simplicity only one type of receptor is shown for each cartoon. Ligands (blue pentagons) bind to receptors either directly (C, E) or indirectly via BPs (green ovals; D, F). A rapid increase in ligand binding above the adapted level of receptor methylation inactivates receptors and the associated kinase CheA, bringing them from "*on*" (red shades) to "*off*" (blues shades) state. At low concentrations, both types of ligands do not saturate their binding sites and mediate similar responses (C, D). For directly binding ligands, the sensitivity of response at high ambient concentrations is retained due to increased receptor methylation (yellow ovals), which effectively reduces ligand binding affinity of receptors in the adapted state and enables sensing further increases in ligand concentration (E; see main text for details). Thus, response is lost only upon the failure of the

adaptation system, as shown in (A). In contrast, response to indirectly binding ligands is limited at high ambient concentration by saturation of BP, whose ligand binding affinity cannot be adjusted by the adaptation system operating on receptors. Thus, response terminates well before the failure of adaptation.

Figure S4. Quantification of relative receptor levels. To obtain a single electrophoretic band for each receptor, the quantification was performed in *cheR cheB* mutants (VS275 or its derivative SN23), where all native receptors are present in a half-amidated state with defined mobility. (A) Strategy used to determine specificity of the antibody. Cells, each expressing a particular receptor-YFP fusion from one of the pTrc-based plasmids listed in Table SII, were grown to OD_{600} of 0.45 (I). Relative expression levels of individual receptor-YFP fusions were quantified using FACScan (II). Cell lysates for immunoblot analysis were then adjusted to the same relative receptor-YFP concentration according to the FACS value of the respective culture (III). Immunoblots using monoclonal αGFP antibody served as a control for possible degradation of receptor-YFP fusions, with examples shown for Trg- and Tap-YFP (IV) and to ensure that each sample contains the same concentration of receptor-YFP fusion (V). Next, the relative specificities of αTar (VI) and αTrg (VII) antibodies for receptors were quantified by hybridizing them with defined amounts of receptor-YFP fusions. (B) Resulting specificities of αTar and αTrg antibodies, plotted relative to their specificities for Tsr. αTar (VI) recognized both major receptors about equally [Tar/Tsr $_{\alpha Tar}$: 1.39 ± 0.23], but recognized other receptors less efficiently. In contrast, αTrg (VII) recognizes all receptors about equally [Trg/Tsr $_{\alpha Trg}$: 1.64 ± 0.13; Tap/Tsr $_{\alpha Trg}$: 1.23 ± 0.08]. (C) Determination of native receptor levels using *cheR cheB* mutants. The native Tar/Tsr ratio was determined from αTar blots using strain VS275 (top). Due to the poor recognition of Trg by αTar and the lower native expression of Trg, there was no significant interference of the Trg receptor band with quantification of Tar. Band intensities for all native receptors were similar on αTrg blots

(bottom). Since the Trg and Tar bands strongly interfere in this case, we quantified the ratio of Tap/Tsr from strain VS275 (Tar^+) and the ratio of Trg/Tsr from strain SN23 (VS275 Δ*tar*). (D) Ratios of the native receptor levels for LJ110 derivatives were calculated by dividing the ratio of native receptor bands (C) by the relative antibody specificity (B). (E) Ratios of native receptor levels determined as described before but for *cheR cheB* derivatives of RP437 (VS149 [Tar^+] and RBB1041 [Δ(*tar tap*)]). Error bars indicate standard errors. See *Supplementary methods* for more details.

Figure S5. Estimation of absolute receptor numbers. To estimate the absolute number of receptors we used cultures expressing varying levels of YFP, as well as non-fluorescent control cells (I). Cells were lyzed by incubation with 1 mg/ml lysozyme and subsequent sonication. Lysate of non-fluorescent cells was used as a background to calibrate a fluorimeter using purified YFP of known concentration (II). This calibration curve was then used to obtain the YFP concentration in a given culture analyzed with the fluorimeter (II). Same cultures were also analyzed using FACS (III). Since the concentration of bacterial cells in the analyzed cultures (III) and the number of molecules in the purified YFP solution are known, the number of YFP molecules per cell can be directly correlated with the FACS values (IV). This in turn can be used to estimate the absolute number of Tsr by comparing intensities of Tsr-YFP and native Tsr bands in the linear range using immunoblot with αTar antibody (V). The obtained absolute number of Tsr can be used to calculate the absolute number of other receptors using the ratios of native receptors given in Fig. S4 D. See *Supplementary methods* for more details.

Figure S6. Dependence of the relative expression of Tsr, Trg and Tap on the optical density of the culture. Receptor ratios were quantified at different OD_{600} in SN23 (Trg/Tsr) and VS275 (Tap/Tsr) grown under standard conditions using immunoblotting with αTrg

antibody as in Fig. S4B. Data are from one experiment each. See *Supplementary methods* for more details.

Figure S7. Dynamic range for serine in *tsr* mutant. Dynamic range was determined as in Fig. 2A. The wild-type dynamic range for serine is shown as a reference. Error bars indicate standard errors.

Figure S8. Dependence of the dynamic range on binding protein and receptor expression. (A) Dependence of the dynamic range for Pro-Leu on the expression level of DppA. Expression levels correspond to the first four and the last point in Fig. 4A. (B and C) Comparison of the dynamic range for maltose (B) and ribose (C) in wild-type cells expressing RbsB and MalE at maximum induction from salicylate-inducible plasmids with the wild-type range (WT). (D) Dynamic range of the response to galactose at the wild-type level of Trg and with Trg overexpressed about 18-fold. Error bars indicate standard errors. Data in (D) are from one experiment.

Figure S9. Differences in Tar methylation pattern upon stimulation with directly and indirectly binding ligands. (A) An immunoblot with αTar antibody for LJ110 cells that were pre-adapted in buffer (lane 1) and subsequently stimulated with 1 mM maltose (lane 2), 1 mM MeAsp (lane 3) or 1 mM aspartate (lane 4) for 10 min. Since maltose and aspartate are metabolized rapidly, 1 mM attractant was added every minute. Positions of differently methylated Tar receptors were estimated from Δ*cheR*, Δ*cheR cheB*, and Δ*cheB* mutants that are expected to carry Tar receptors in Tar_{EEEE}, Tar_{QEQE}, and Tar_{QEmQEm} states, were glutamine (Q) mimics effects of methylated glutamate (Em) on activity and mobility on the gel. Note that the running behaviour of glutamine may slightly differ from that of the methylated glutamate. (B) Intensity profile of the immunoblot shown in (A). Profiles were measured for

each lane in (A) with a stripe of defined area applied along the run distance of the gel using ImageJ software. For better comparison, the obtained values were normalized to the integral intensity of all bands within the respective lane. The extent of methylation upon ligand stimulation can be followed as an increase of relative intensity of bands corresponding to high modification. This effect is much more pronounced for the directly binding ligands aspartate and MeAsp than for the indirectly binding ligand maltose. A slight increase in methylation of the non-cognate receptor Tsr indicates its cross-methylation due to interactions between receptors. Note that in the middle part of the profile, bands corresponding to highly methylated Tsr and unmethylated Tar receptors overlap.

Figure S1

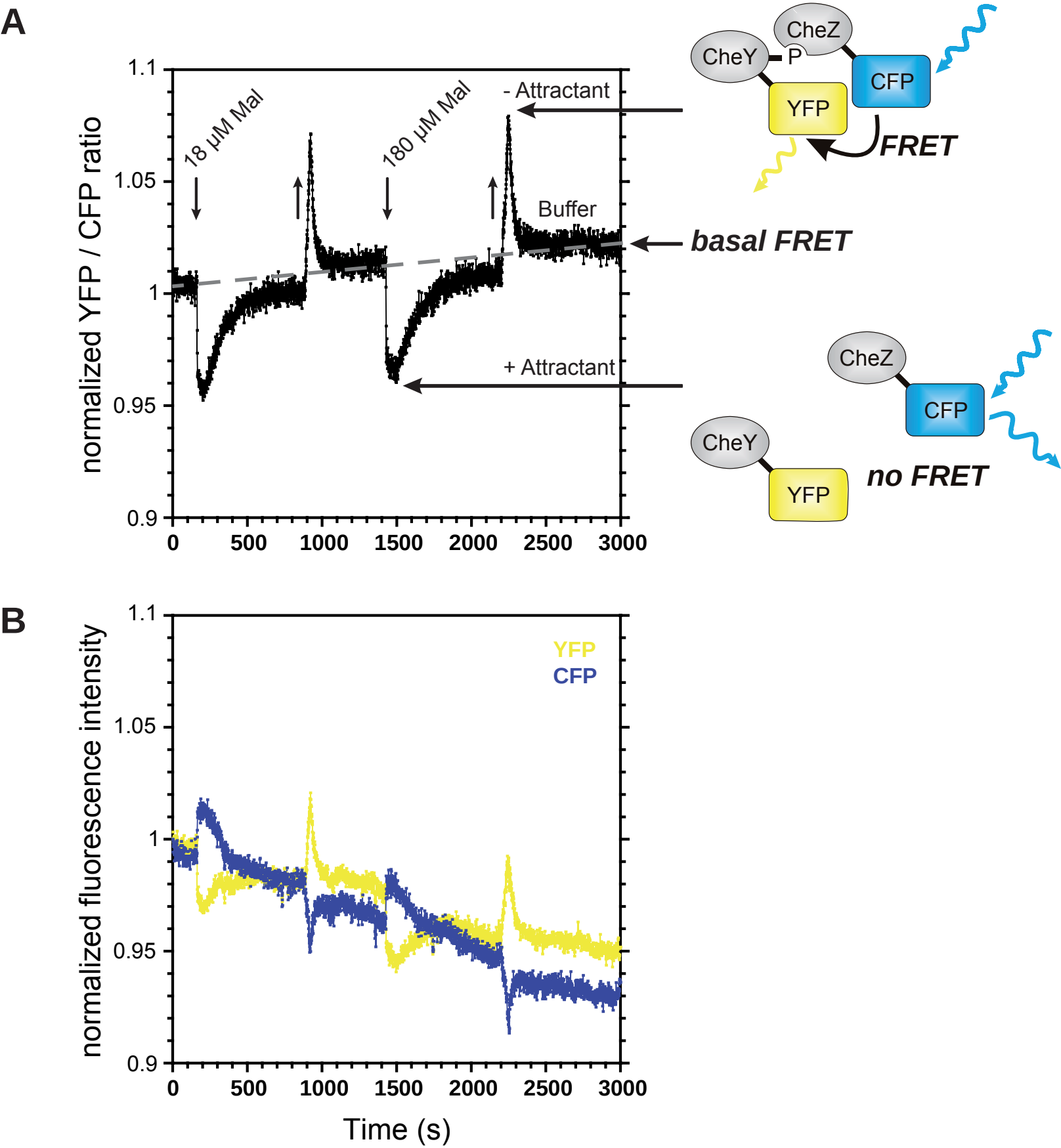
A
normalized YFP / CFP ratio
1.1
1.05
1
0.95
0.9
0
500
1000
1500
2000
2500
3000
18 µM Mal
180 µM Mal
- Attractant
Buffer
+ Attractant
basal FRET
CheZ
CheY
P
CFP
YFP
FRET
CheZ
CFP
CheY
YFP
no FRET
B
normalized fluorescence intensity
YFP
CFP
Time (s)

Figure S2

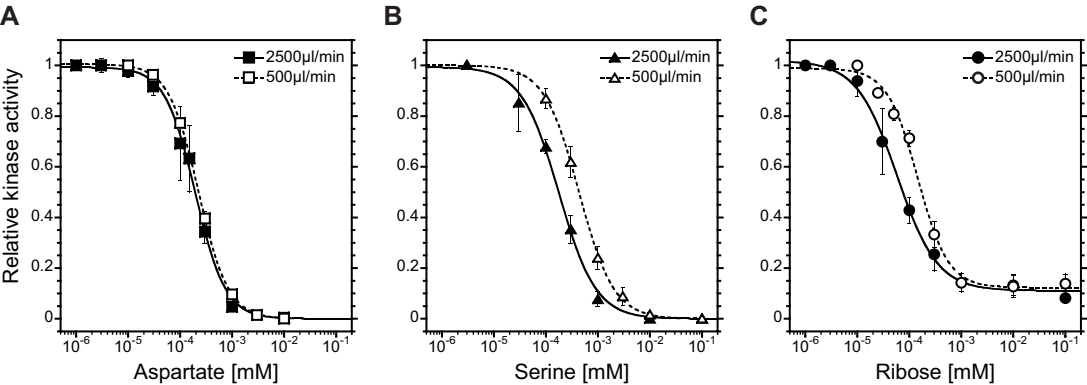
A
B
C
Relative kinase activity
2500µl/min
500µl/min
Aspartate [mM]
Serine [mM]
Ribose [mM]

Figure S3

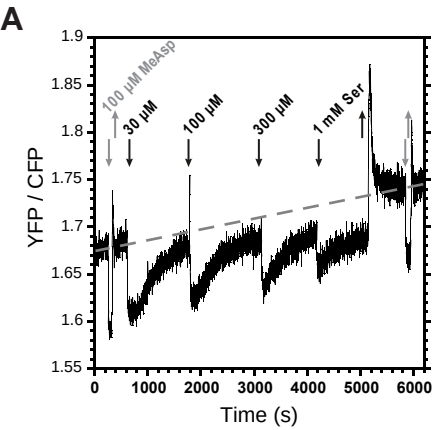
A
100 µM MeAsp
30 µM
100 µM
300 µM
1 mM Ser
YFP / CFP
Time (s)

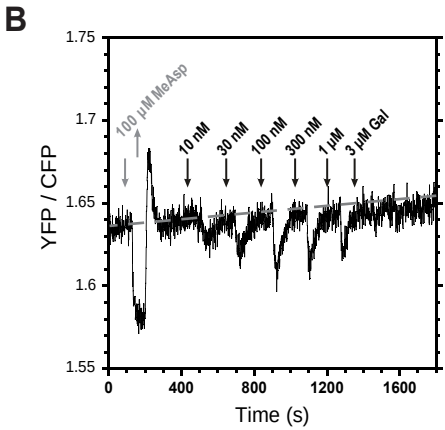
B
100 µM MeAsp
10 nM
30 nM
100 nM
300 nM
1 µM
3 µM Gal
YFP / CFP
Time (s)

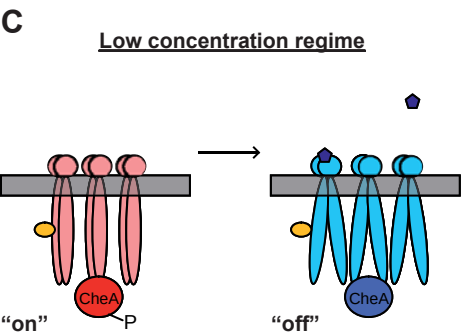
C
Low concentration regime
CheA
P
"on"
"off"

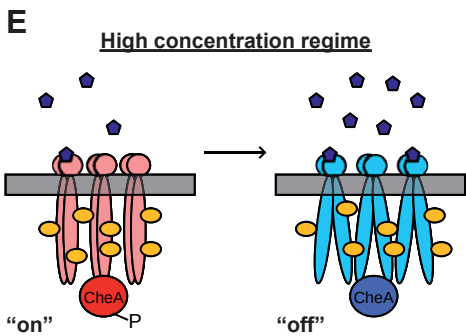
E
High concentration regime
CheA
P
"on"
"off"

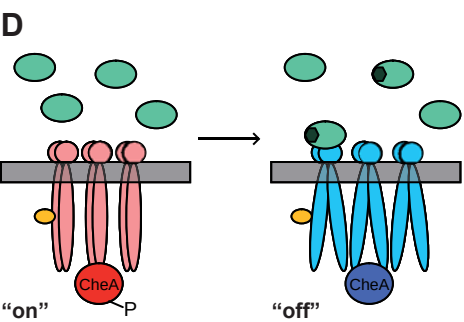
D
CheA
P
"on"
"off"

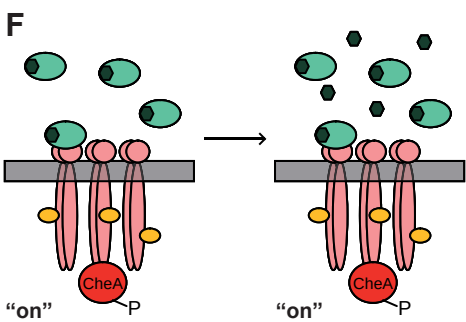
F
CheA
P
"on"
"on"

Figure S4

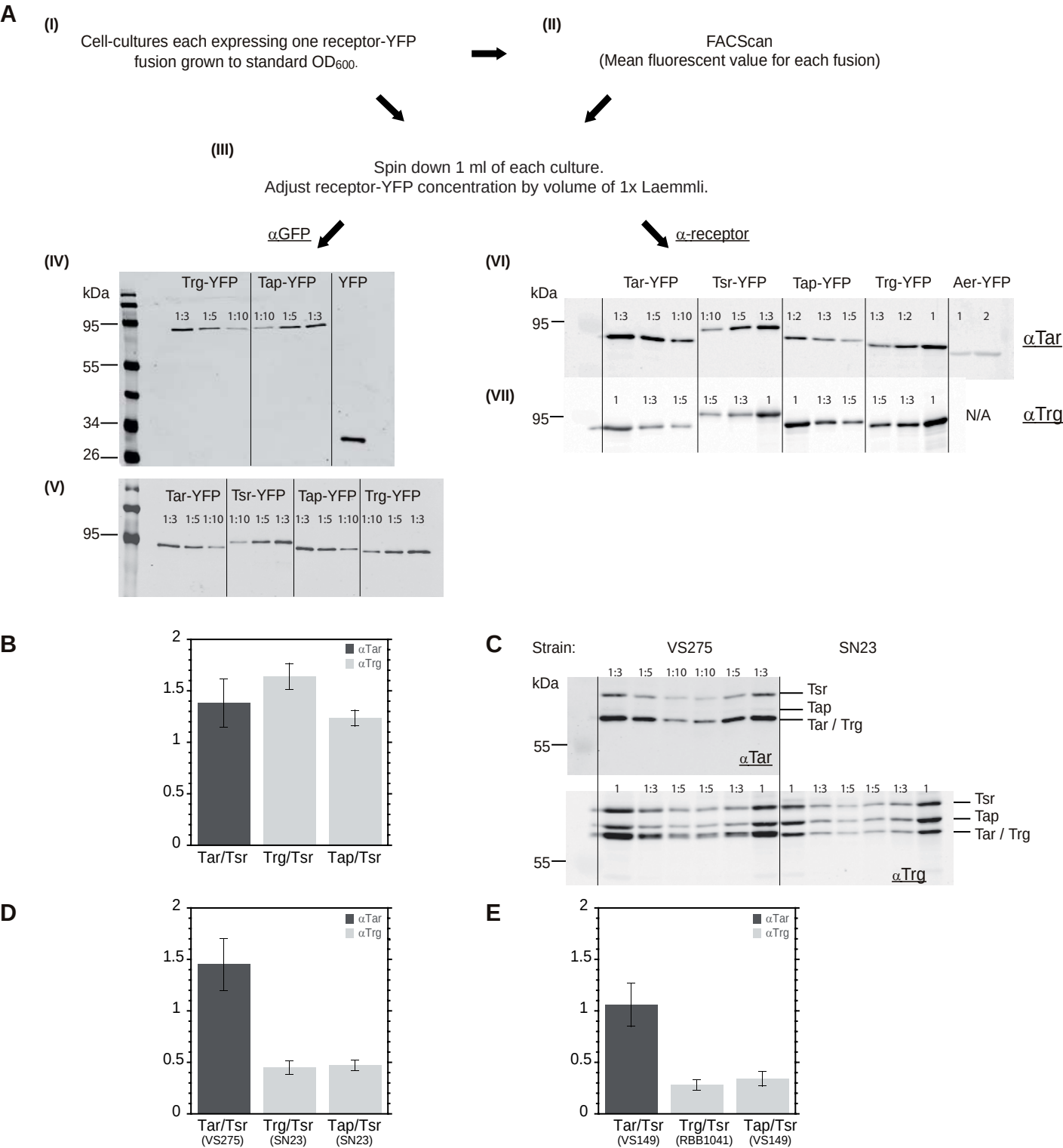
A
(I)
Cell-cultures each expressing one receptor-YFP fusion grown to standard OD600.
(II)
FACScan
(Mean fluorescent value for each fusion)
(III)
Spin down 1 ml of each culture.
Adjust receptor-YFP concentration by volume of 1x Laemmli.
αGFP
α-receptor
(IV)
kDa
95
55
34
26
Trg-YFP
Tap-YFP
YFP
1:3 1:5 1:10 1:10 1:5 1:3
(V)
95
Tar-YFP
Tsr-YFP
Tap-YFP
Trg-YFP
1:3 1:5 1:10 1:10 1:5 1:3 1:3 1:5 1:10 1:10 1:5 1:3
(VI)
kDa
95
Tar-YFP
Tsr-YFP
Tap-YFP
Trg-YFP
Aer-YFP
1:3 1:5 1:10 1:10 1:5 1:3 1:2 1:3 1:5 1:3 1:2 1 1 2
αTar
(VII)
95
1 1:3 1:5 1:5 1:3 1 1 1:3 1:5 1:5 1:3 1
N/A
αTrg
B
2
1.5
1
0.5
0
αTar
αTrg
Tar/Tsr
Trg/Tsr
Tap/Tsr
C
Strain:
VS275
SN23
kDa
55
1:3 1:5 1:10 1:10 1:5 1:3
Tsr
Tap
Tar / Trg
αTar
1 1:3 1:5 1:5 1:3 1 1 1:3 1:5 1:5 1:3 1
Tsr
Tap
Tar / Trg
55
αTrg
D
2
1.5
1
0.5
0
αTar
αTrg
Tar/Tsr
(VS275)
Trg/Tsr
(SN23)
Tap/Tsr
(SN23)
E
2
1.5
1
0.5
0
αTar
αTrg
Tar/Tsr
(VS149)
Trg/Tsr
(RBB1041)
Tap/Tsr
(VS149)

Figure S5

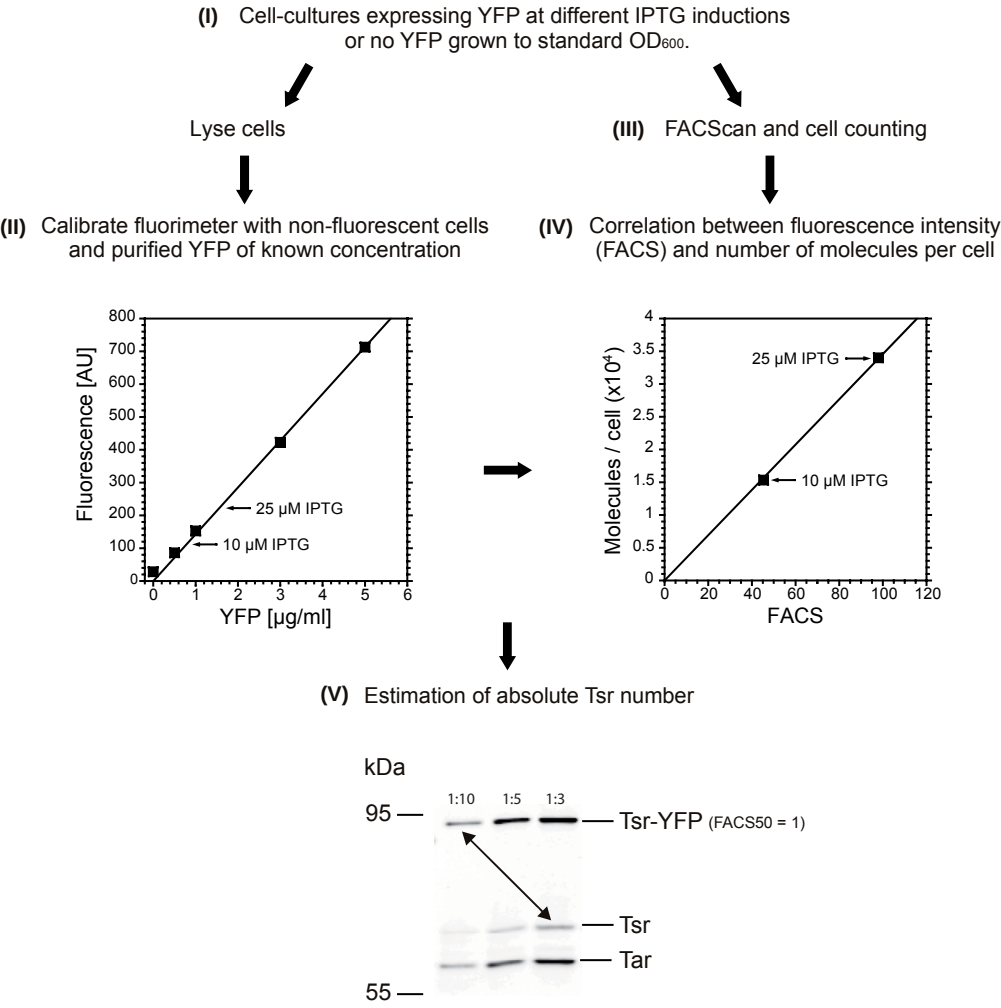
(I) Cell-cultures expressing YFP at different IPTG inductions or no YFP grown to standard OD600.
Lyse cells
(III) FACScan and cell counting
(II) Calibrate fluorimeter with non-fluorescent cells and purified YFP of known concentration
(IV) Correlation between fluorescence intensity (FACS) and number of molecules per cell
Fluorescence [AU]
YFP [µg/ml]
25 µM IPTG
10 µM IPTG
Molecules / cell (x10^4)
FACS
(V) Estimation of absolute Tsr number
kDa
95
55
1:10
1:5
1:3
Tsr-YFP (FACS50 = 1)
Tsr
Tar

Figure S6

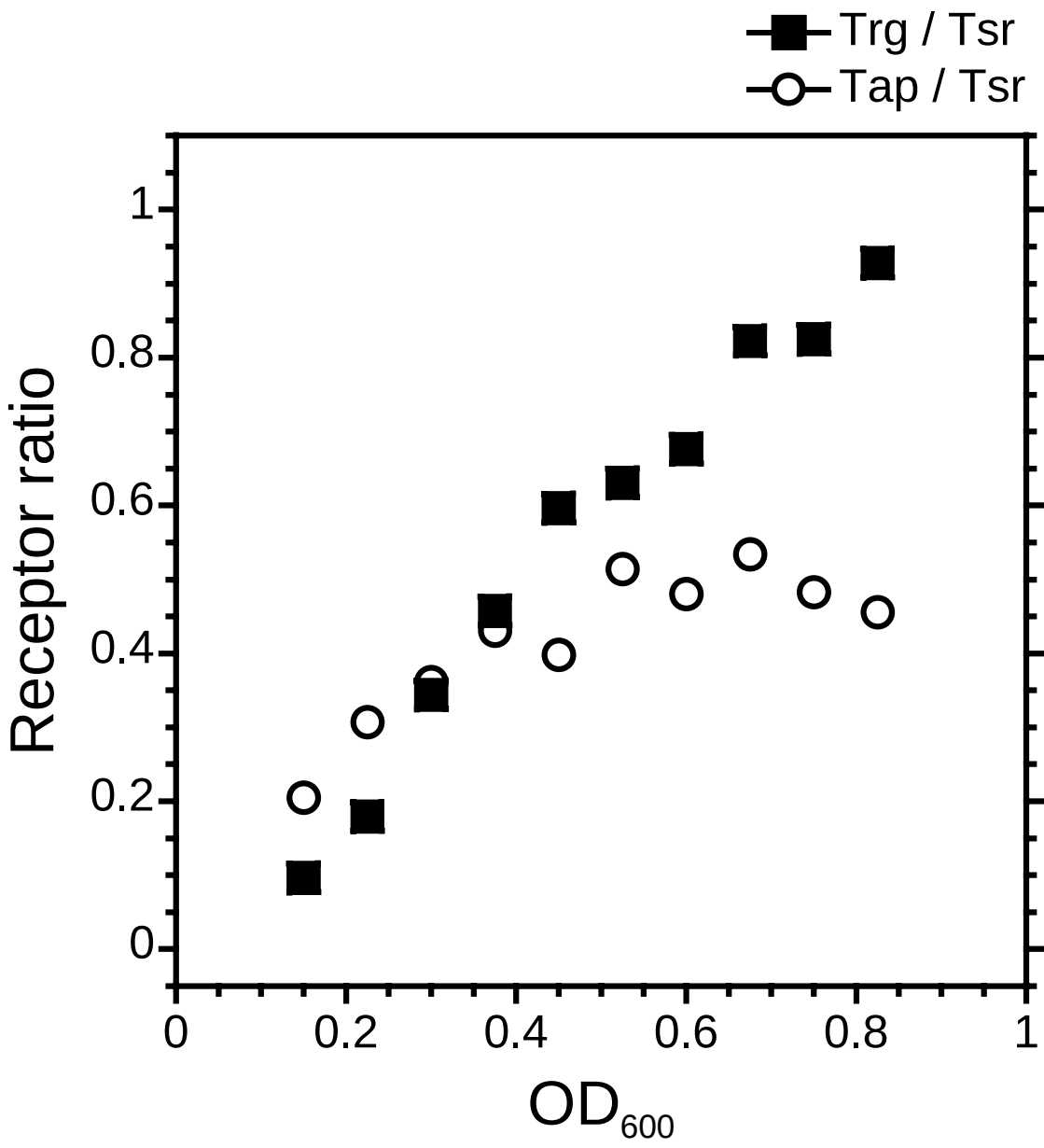
Trg / Tsr
Tap / Tsr
Receptor ratio
0
0.2
0.4
0.6
0.8
1
0
0.2
0.4
0.6
0.8
1
OD600

Figure S7

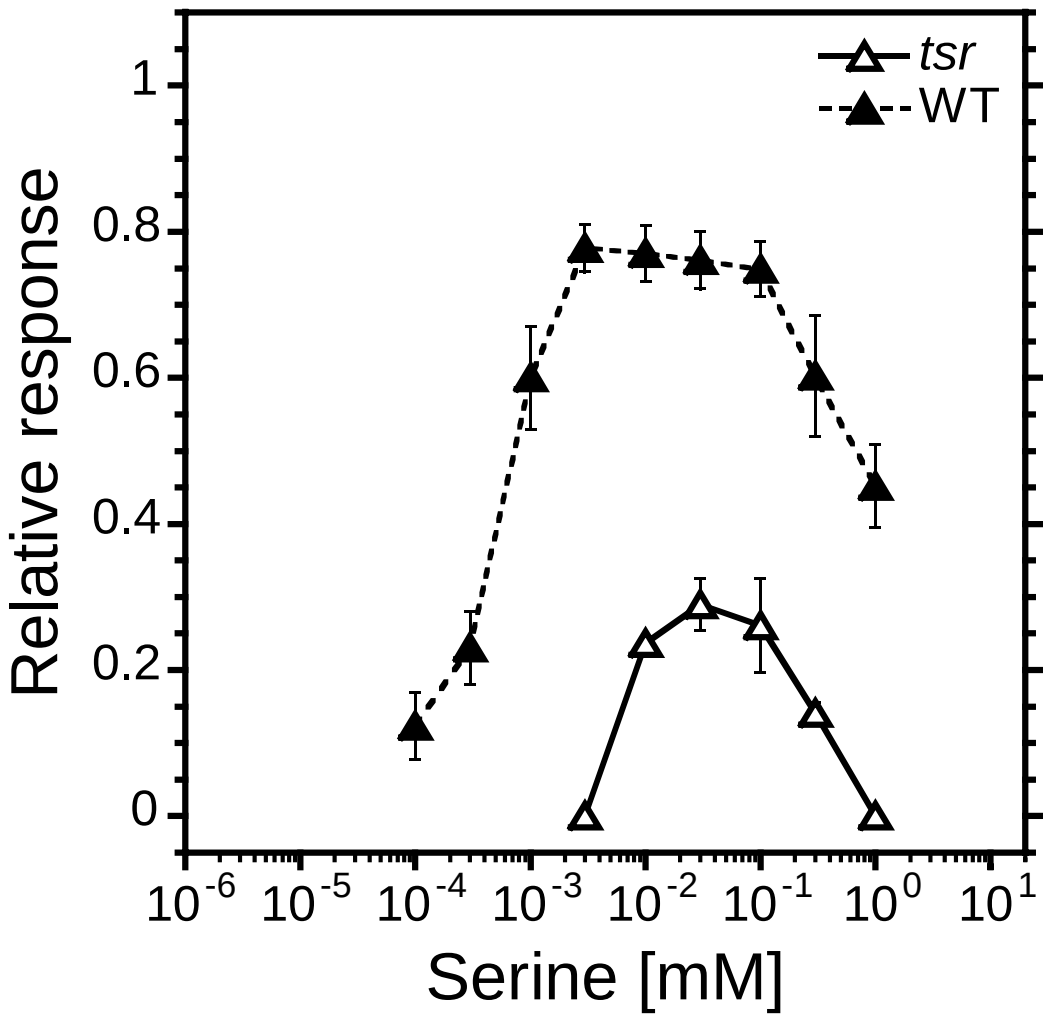
tsr
WT
Relative response
1
0.8
0.6
0.4
0.2
0
10-6 10-5 10-4 10-3 10-2 10-1 100 101
Serine [mM]

Figure S8

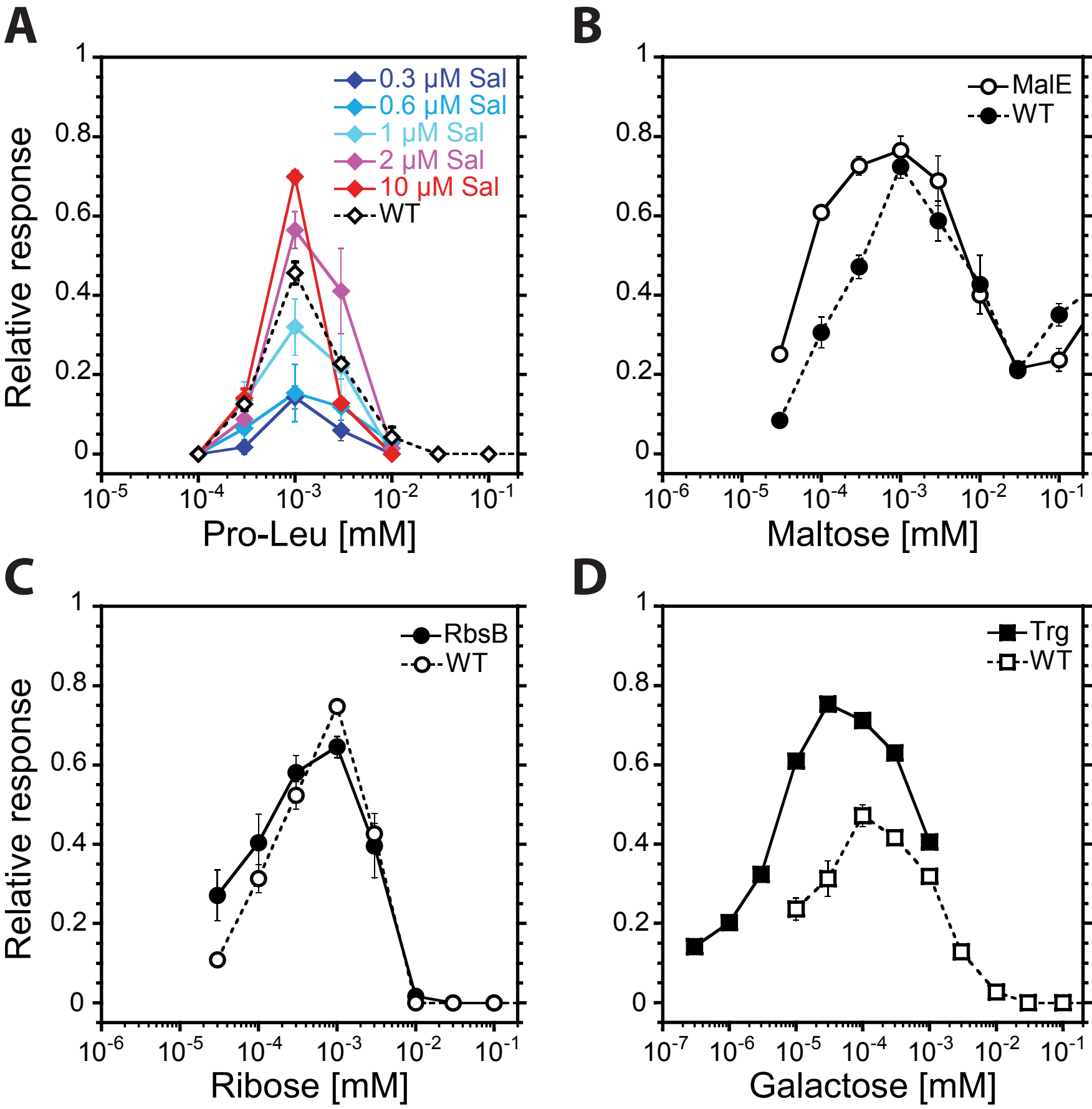
A
B
C
D
Relative response
Pro-Leu [mM]
0.3 µM Sal
0.6 µM Sal
1 µM Sal
2 µM Sal
10 µM Sal
WT
MalE
WT
Maltose [mM]
RbsB
WT
Ribose [mM]
Trg
WT
Galactose [mM]

Figure S9

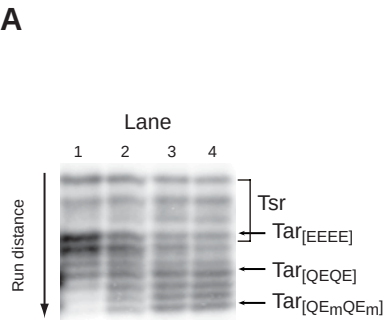
A
Lane
1
2
3
4
Run distance
Tsr
Tar[EEEE]
Tar[QEQE]
Tar[QEmQEm]

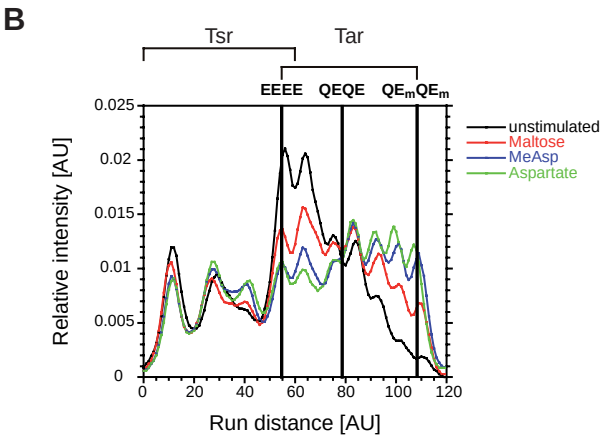
B
Tsr
Tar
EEEE
QEQE
QEmQEm
unstimulated
Maltose
MeAsp
Aspartate
Relative intensity [AU]
0.025
0.02
0.015
0.01
0.005
0
0
20
40
60
80
100
120
Run distance [AU]

Table SI. Response parameters for individual ligands and receptor expression levels

Ligand (Receptor)	$S_T \times 10^3$ mM^{-1} (wild-type)[a]	$S_T \times 10^3$ mM^{-1} (maximal BP induction)	$S_T \times 10^3$ mM^{-1} (maximal receptor induction)	Ambient concentration[b]	S_R^P (wild-type)[c]	S_R^P (maximal BP induction)	Relative receptor level[d]	Receptor fraction in the total pool	$S_T^{max} \times 10^3$ mM^{-1} (wild-type)[e]	$S_R^{Pmax} \times 10^3$ mM^{-1} (calculated)[f]
Serine (Tsr)	6.1 ± 0.8 (2.1 ± 0.3)	-	N/A	30 µM	6.4 ± 0.2	-	1.0	0.297 ± 0.024	21 ± 3	22 ± 2
AiBu (Tsr)	0.021 ± 0.007 (0.0077 ± 0.0011)	-	N/A	1 mM	2.1 ± 0.2	-	1.0	0.297 ± 0.024	0.071 ± 0.024	7.2 ± 0.9
Asp (Tar)	5.2 ± 0.9 (4.5 ± 0.2)	-	N/A	3 µM	5.1 ± 0.2	-	1.45 ± 0.25	0.430 ± 0.082	12 ± 3	12 ± 2
MeAsp (Tar)	0.45 ± 0.03 (0.25 ± 0.03)	-	0.52 ± 0.04	100 µM	4.5 ± 0.4	-	1.45 ± 0.25	0.430 ± 0.082	1.0 ± 0.2	10 ± 2
Maltose (Tar)	7.9 ± 1.4 (5.6 ± 0.4)	N/A (31 ± 7)	-	300 nM	0.92 ± 0.09	2.3 ± 0.2	1.45 ± 0.25	0.430 ± 0.082	18 ± 5	5.3 ± 1.2
				1 µM	1.6 (n=1)	2.3 ± 0.2				5.2 ± 1.1
Galactose (Trg)	67 ± 1 (44 ± 3)	N/A (42 ± 4)	867 ± 150	30 nM	0.37 ± 0.04	0.36 ± 0.07	0.45 ± 0.07	0.134 ± 0.022	500 ± 82	2.7 ± 0.7
				100 nM	0.36 ± 0.02	0.48 (n=1)				3.6 ± 0.6
Ribose (Trg)	16 ± 3 (6.3 ± 0.8)	N/A (22 ± 3)	91 ± 9	300 nM	1.3 ± 0.2	1.2 ± 0.2	0.45 ± 0.07	0.134 ± 0.022	119 ± 30	8.9 ± 1.9

				1 µM	1.6 ± 0.1	1.6 ± 0.3				12 ± 3
Pro-Leu (Tap)	2.8 ± 0.4	N/A	N/A	300 nM	0.28 ± 0.09	1.1 ± 0.2	0.47 ± 0.05	0.139 ± 0.019	20 ± 4	7.7 ± 1.6
	(1.2 ± 0.1)	(2.6 ± 0.1)								
				600 nM	N/A	0.77 (n=1)				5.5 ± 0.8
				1 µM	0.38 ± 0.08	N/A				N/A

Errors indicate standard errors.

[a] Threshold sensitivity, calculated as EC_{50}^{-1}; values in brackets were determined from measurements performed at a flow rate of 500 µl/min.

[b] Ambient concentrations were chosen around the peak of the dynamic range (see Fig. 1B and C).

[c] Response sensitivity at the peak of the dynamic range, measured as a relative change in kinase activity over relative change in ligand concentration.

[d] Calculated from immunoblots relative to the level of Tsr (appr. 6000 copies per cell; see Fig. S5).

[e] Maximal threshold sensitivity, calculated as S_T divided by receptor fraction.

[f] Maximal response sensitivity, calculated as S_R^P divided by receptor fraction; S_R^P values at maximal binding protein induction were used for the indirect binding.

Table SII. Strains, plasmids and primers used in this study.

Strains

Strain	Relevant genotype	Reference
LJ110	W3110 Fnr^+ (wild type)	Zeppenfeld et al, 2000
SN1	LJ110 Δ(*cheY cheZ)*	This work
SN11	LJ110 Δ(*cheY cheZ)* Δ*tsr::Tn5* (Kan^R)	This work
SN25	LJ110 Δ(*cheY cheZ)* Δ*tar*	This work
SN27	LJ110 Δ(*cheY cheZ)* Δ*dppA*	This work
SN28	LJ110 Δ(*cheY cheZ)* Δ*mglB*	This work
SN31	LJ110 Δ(*cheY cheZ)* Δ*malE*	This work
VS275	LJ110 Δ(*cheR cheB cheY cheZ)*	This work
SN23	LJ110 Δ(*cheR cheB cheY cheZ)* Δ*tar*	This work
VS149	RP437 Δ(*cheR cheB cheY cheZ)*	Sourjik & Berg, 2004
RBB1041 (VS305)	RP437 Δ(*cheA cheW tar tap cheR cheB cheY cheZ*)::Zeo^R	Abouhamad et al, 1998
VS124	RP437 Δ(*cheB cheY cheZ)*	Sourjik & Berg, 2002
VS126	RP437 Δ(*cheR*)	Sourjik & Berg, 2000
JW1875	MG1655 *tar::kan*	Baba et al, 2006
JW2137	MG1655 *mglB::kan*	Baba et al, 2006
JW3513	MG1655 *dppA::kan*	Baba et al, 2006
JW3994	MG1655 *malE::kan*	Baba et al, 2006

VS139	RP437 Δ(*cheY cheZ)* Δ*tsr::Tn5* (Kan^R)	V. Sourjik

Plasmids

Plasmid		Primers used for cloning	
pAMPts	Cloning vector; ts origin of replication; Amp^R		Phillips, 1999
pVS22	Δ(*cheY cheZ)* construct; pAMPts derivative		Sourjik & Berg, 2002
pVS84	Δ(*cheR cheB cheY cheZ)* construct; pAMPts derivative		Sourjik & Berg, 2004
pTrc99a	Expression vector; pBR ori, *trc* promoter; Amp^R		Amann et al, 1988
pDK66	Expression vector for cloning of C-terminal YFP fusions; pTrc99a derivative with weaker RBS than the original pTrc99a		Kentner et al, 2006
pVS88	*cheY-eyfp cheZ-ecfp*; pTrc99a derivative		Sourjik & Berg, 2004
pSN57	*tap-eyfp*; pTrc99a derivative	DK74/DK75	This work
pSN42	*trg-eyfp*; pTrc99a derivative	DK72/DK73	This work
pDK80	*tsr-eyfp*; pDK66 derivative	DK6a/DK6b	Kentner & Sourjik, 2009
pDK58	*tar-eyfp*; pDK66 derivative	DK5a/DK5b	Kentner et al, 2006
pKG110	Expression vector; p15A ori; *nahG* promoter; Cm^R		gift from S. Parkinson, University of Utah
pSN43 [a]	*trg*; pKG110 derivative	SN35_fw/SN32_rev	This work
pSN72 [b]	*dppA*; pKG110 derivative	SN47_fw/SN47_rev	This work
pSN78 [b]	*malE*; pKG110 derivative	SN51_fw/SN51_rev	This work
pSN76 [b]	*mglB*; pKG110 derivative	SN50_fw/SN50_rev	This work
pSN77 [b]	*rbsB*; pKG110 derivative	SN53_fw/SN53_rev	This work
pLC113	*tar* [QEQE]; pKG110 derivative		Ames et al, 2002
pVS123	*tar* [QEQE]; pLC113 derivative		Sourjik & Berg, 2004
pRR31	Expression vector; p15A ori; *nahG* promoter; Cm^R		Studdert & Parkinson, 2005
pVS118	*eyfp*; pRR31 derivative		This work

[a] *trg* was cloned via *Nde*I/*BamH*I with the *E. coli* Shine Dalgarno consensus RBS included in the forward primer.

[b] Primer SN47_fw includes the prokaryotic Shine-Dalgarno consensus RBS between a *Nde*I and *Spe*I restriction sites. The resulting plasmid pSN72 was used for cloning of pSN76, pSN77 and pSN78 via *Spe*I/*BamH*I.

Primers

Primer	Target gene	Sequence
SN47_fw	*dppA*	5'-TACTATCATATG**AGGAGG**ACTAGTAATGCGTATTTCCTTG-3'
		*Nde*I **RBS** *Spe*I
SN47_rev		5'-ATAGTAGGTACCTTATTCGATAGAGACG-3'
		*Kpn*I
SN51_fw	*malE*	5'-TACTATACTAGTATGAAAATAAAAACAGGTGC-3'
		*Spe*I
SN51_rev		5'-ATAGTAGGATCCTTACTTGGTGATACGAGTC-3'
		*Bam*HI
SN50_fw	*mglB*	5'-TACTATACTAGTatgAATAAGAAGGTGTTAAC-3'
		*Spe*I
SN50_rev		5'-ATAGTAGGATCCTTATTTCTTGCTGAATTCAG-3'
		*Bam*HI
SN53_fw	*rbsB*	5'-TACTATACTAGTATGAACATGAAAAAACTGGC-3'
		SpeI
SN53_rev		5'-ATAGTAGGATCCCTACTGCTTAACAACCAG-3'
		*Bam*HI
SN35_fw	*trg*	5'-TACTATCATATGT**AGGAGGT**CGGTAATGAATACAACTCCCTCAC-3'
		*Nde*I **RBS**
SN32_rev		5'-ATAGTAGGATCCTCACACCGTAGCGAAACTAAC-3'
		*Bam*HI
DK5a	*tar*	5'-ATGCCATGGGTATGATTAACCGTATCCGCG-3'
		*Nco*I
DK5b		5'-GATGGATCCAAATGTTTCCCAGTTTGGATC-3'
		*Bam*HI
DK6a	*tsr*	5'-ATGCCATGGGTATGTTAAAACGTATCAAAATTG-3'
		*Nco*I
DK6b		5'-GCATGGATCCAAATGTTTCCCAGTTCTCC-3'
		*Bam*HI
DK72	*trg*	5'-ATATACCATGGGCAATACAACTCCCTCAC-3'
		*Nco*I
DK73		5'-TATATGGATCCCACCGTAGCGAAACTAAC-3'

		*Bam*HI
DK74	*tap*	5'-ATATACCATGGGCTTTAATCGTATTCGAATTTCG-3'
		*Nco*I
DK75		5'-TATATGGATCCGGATACCACTGGCGCAATTTG-3'
		*Bam*HI
Vic146	binds ~270bp in *cheW*	5'-ACACGGGAATTCTCGTCCTGAATCTCGG-3'
Vic113	binds ~500bp in *cheR*	5'-ATGGCGAATTCATACCGCTTCTGGC-3'

Supplementary references

Abouhamad WN, Bray D, Schuster M, Boesch KC, Silversmith RE, Bourret RB (1998) Computer-aided resolution of an experimental paradox in bacterial chemotaxis. *J Bacteriol* **180:** 3757-3764

Amann E, Ochs B, Abel KJ (1988) Tightly regulated tac promoter vectors useful for the expression of unfused and fused proteins in *Escherichia coli*. *Gene* **69:** 301-315

Ames P, Studdert CA, Reiser RH, Parkinson JS (2002) Collaborative signaling by mixed chemoreceptor teams in *Escherichia coli*. *Proc Natl Acad Sci U S A* **99:** 7060-7065

Baba T, Ara T, Hasegawa M, Takai Y, Okumura Y, Baba M, Datsenko KA, Tomita M, Wanner BL, Mori H (2006) Construction of *Escherichia coli* K-12 in-frame, single-gene knockout mutants: the Keio collection. *Mol Syst Biol* **2:** 2006 0008

Kentner D, Sourjik V (2009) Dynamic map of protein interactions in the Escherichia coli chemotaxis pathway. *Mol Syst Biol* **5:** 238

Kentner D, Thiem S, Hildenbeutel M, Sourjik V (2006) Determinants of chemoreceptor cluster formation in *Escherichia coli*. *Mol Microbiol* **61:** 407-417

Phillips GJ (1999) New cloning vectors with temperature-sensitive replication. *Plasmid* **41:** 78-81

Sourjik V, Berg HC (2000) Localization of components of the chemotaxis machinery of *Escherichia coli* using fluorescent protein fusions. *Mol Microbiol* **37:** 740-751

Sourjik V, Berg HC (2002) Receptor sensitivity in bacterial chemotaxis. *Proc Natl Acad Sci U S A* **99:** 123-127

Sourjik V, Berg HC (2004) Functional interactions between receptors in bacterial chemotaxis. *Nature* **428:** 437-441

Studdert CA, Parkinson JS (2005) Insights into the organization and dynamics of bacterial chemoreceptor clusters through *in vivo* crosslinking studies. *Proc Natl Acad Sci U S A* **102:** 15623-15628

Zeppenfeld T, Larisch C, Lengeler JW, Jahreis K (2000) Glucose transporter mutants of *Escherichia coli* K-12 with changes in substrate recognition of IICB(Glc) and induction behavior of the ptsG gene. *J Bacteriol* **182:** 4443-4452

Supplementary model for

Differences in signalling by directly and indirectly binding ligands in bacterial chemotaxis

Silke Neumann, Clinton H. Hansen, Ned S. Wingreen and Victor Sourjik

Free-energy model for receptor teams

Within the Monod-Wyman-Changeux (MWC) model for chemoreceptors, a tightly coupled team of receptors turns on or off as a whole, with the activity A, *i.e.* the probability of being on, determined solely by the free-energy difference between the on and off states summed over all receptors in the team,

$$A = \frac{1}{1 + e^{\sum_r n_r f_r}}, \tag{1}$$

where f_r is the free-energy difference for receptors of type r and n_r is the number of such receptors in the team [1–4]. Receptors can be inactivated by chemoeffectors by binding ligand directly, or binding to a BP that binds ligand. For a receptor that directly binds ligand, a ligand molecule can be bound by the receptor in either the receptor's on or off state, albeit with different affinities. Therefore for each receptor, the four possible configurations and their free energies are: on with no ligand bound, $E_r^{\rm on}$, on with ligand bound, $E_r^{\rm on} - \log\left([{\rm L}]/K_r^{\rm on}\right)$, off with no ligand bound, $E_r^{\rm off}$, and off with ligand bound, $E_r^{\rm off} - \log\left([{\rm L}]/K_r^{\rm off}\right)$, with all energies expressed in units of the thermal energy $k_B T$. Here $K_r^{\rm on}$ and $K_r^{\rm off}$ are the binding constants in the on and off states for a specific type of receptor r. The free-energy difference between on and off receptor states is therefore

$$f_r = \epsilon_r + \log \frac{1 + \frac{[{\rm L}]}{K_r^{\rm off}}}{1 + \frac{[{\rm L}]}{K_r^{\rm on}}}, \tag{2}$$

where we have defined $\epsilon_r = E_r^{\rm on} - E_r^{\rm off}$ as the offset energy in the absence of ligand.

Minor receptors do not bind chemoeffectors directly. Instead, the chemoeffector ligand binds to a periplasmic protein, which binds to the receptor. The periplasmic binding protein (BP) can assume an open or closed configuration. The open state is strongly favored in the absence of ligand and the closed state is strongly favored by ligand binding. Here we calculate the free-energy difference between the on and off states of a minor receptor in the presence of periplasmic BP at concentration [BP] and ligand its at concentration [L]. We assume that binding to the receptor depends only on the BP conformation, independent of the presence of a bound ligand (*i.e.* the receptor cannot distinguish a closed BP with ligand from a closed BP without ligand). In the absence of ligand, there is a free-energy offset ϵ_{BP} between the open and closed states of the BP. Similarly, in the absence of BP, there is a free-energy offset ϵ_r between the on and off states of the receptor. The BP binds ligand with a dissociation

constant K_{BP}^{open} in the open state and K_{BP}^{closed} in the closed state. An off receptor binds open and closed BPs with dissociation constants $K_r^{\text{off}-\text{open}}$ and $K_r^{\text{off}-\text{closed}}$, respectively, and, similarly, an on receptor binds BPs with constants $K_r^{\text{on}-\text{open}}$ and $K_r^{\text{on}-\text{closed}}$. Therefore the 2 concentrations and 8 parameters that determine the receptor free-energy difference are [BP], [L], ϵ_r, $K_r^{\text{on}-\text{closed}}$, $K_r^{\text{on}-\text{open}}$, $K_r^{\text{off}-\text{closed}}$, $K_r^{\text{off}-\text{open}}$, ϵ_{BP}, K_{BP}^{open}, and K_{BP}^{closed}. Throughout, we assume that the BP is greatly in excess of its cogante receptor, so that we can neglect titration of the BP due to receptor binding.

A periplasmic BP can assume 4 configurations, closed/open and with/without ligand bound, which have free energies: $E_{BP}^{\text{closed}} - \log\left([\text{L}]/K_{BP}^{\text{closed}}\right)$, E_{BP}^{closed}, $E_{BP}^{\text{open}} - \log\left([\text{L}]/K_{BP}^{\text{open}}\right)$, and E_{BP}^{open}. Therefore, with $\epsilon_{BP} = E_{BP}^{\text{open}} - E_{BP}^{\text{closed}}$, the free-energy difference between the open and closed states of the BP is

$$f_{BP} = f_{BP}^{\text{open}} - f_{BP}^{\text{closed}} = \epsilon_{BP} + \log \frac{1 + \frac{[\text{L}]}{K_{BP}^{\text{closed}}}}{1 + \frac{[\text{L}]}{K_{BP}^{\text{open}}}}, \tag{3}$$

leading to BP concentrations of $[\text{BP}_{\text{open}}] = p_{\text{open}}[\text{BP}] = [\text{BP}]/\left(1 + e^{f_{BP}}\right)$ and $[\text{BP}_{\text{closed}}] = p_{\text{closed}}[\text{BP}] = [\text{BP}]e^{f_{BP}}/\left(1 + e^{f_{BP}}\right)$. This last expression can be simply written in terms of ligand concentration [L] as

$$[\text{BP}_{\text{closed}}] = [\text{BP}]\left[p_0 + (p_\infty - p_0)\left(\frac{[\text{L}]}{[\text{L}] + K_{BP}}\right)\right], \tag{4}$$

where

$$K_{BP} = K_{BP}^{\text{open}} K_{BP}^{\text{closed}} \frac{1 + e^{\epsilon_{BP}}}{K_{BP}^{\text{closed}} + e^{\epsilon_{BP}} K_{BP}^{\text{open}}}, \tag{5}$$

and $p_0 = e^{\epsilon_{BP}}/(1+e^{\epsilon_{BP}})$, $p_\infty = K_{BP}^{\text{open}} e^{\epsilon_{BP}}/(K_{BP}^{\text{closed}} + K_{BP}^{\text{open}} e^{\epsilon_{BP}})$ are the proportions of closed BP in the zero and infinite ligand limits, respectively.

The 3 possible states of the receptor in the on configuration are: on without BP bound, on with a closed BP bound, and on with an open BP bound. The free energies of these states are: E_r^{on}, $E_r^{\text{on}} - \log\left([\text{BP}_{\text{closed}}]/K_r^{\text{on}-\text{closed}}\right)$, $E_r^{\text{on}} - \log\left([\text{BP}_{\text{open}}]/K_r^{\text{on}-\text{open}}\right)$. Therefore the combined on-state free energy is (with a similar expression for the off-state free energy) $f_r^{\text{on}} = E_r^{\text{on}} - \log\left[1 + \frac{[\text{BP}_{\text{closed}}]}{K_r^{\text{on}-\text{closed}}} + \frac{[\text{BP}_{\text{open}}]}{K_r^{\text{on}-\text{open}}}\right]$, and with $E_r^{\text{on}} - E_r^{\text{off}} = \epsilon_r$, the free-energy difference between the on and off states of the receptor is

$$f_r = \epsilon_r + \log \frac{1 + \frac{[\text{BP}_{\text{closed}}]}{K_r^{\text{off}-\text{closed}}} + \frac{[\text{BP}_{\text{open}}]}{K_r^{\text{off}-\text{open}}}}{1 + \frac{[\text{BP}_{\text{closed}}]}{K_r^{\text{on}-\text{closed}}} + \frac{[\text{BP}_{\text{open}}]}{K_r^{\text{on}-\text{open}}}}. \tag{6}$$

We found that there are two different simplifying approximations, either one of which is consistent with the experimental data: (1) receptors only bind closed BP, or (2) receptors only bind BP in the receptor off state. Within the main text, for simplicity, we present results using only Approximation 1, however, for completeness, we present analytical results and data collapses for both approximations below.

Within Approximation 1, the receptor only binds the BP in its closed state and the free-energy difference between the on and off states of the receptor is given by

$$f_r = \epsilon_r + \log \frac{1 + \frac{[\mathrm{BP_{closed}}]}{K_r^{\mathrm{off-closed}}}}{1 + \frac{[\mathrm{BP_{closed}}]}{K_r^{\mathrm{on-closed}}}}. \tag{7}$$

To rewrite this free-energy difference in terms of the ligand concentration [L], we define new parameters $\widetilde{K}_r^{\mathrm{off}} = K_r^{\mathrm{off-closed}}/(p_\infty - p_0)$, $\widetilde{K}_r^{\mathrm{on}} = K_r^{\mathrm{on-closed}}/(p_\infty - p_0)$, and $\widetilde{p}_0 = p_0/(p_\infty - p_0)$, yielding

$$f_r = \epsilon_r + \log \frac{1 + \frac{\widetilde{p}_0[\mathrm{BP}]}{\widetilde{K}_r^{\mathrm{off}}} + \frac{[\mathrm{BP}]}{\widetilde{K}_r^{\mathrm{off}}} \left(\frac{[\mathrm{L}]}{[\mathrm{L}]+K_{BP}} \right)}{1 + \frac{\widetilde{p}_0[\mathrm{BP}]}{\widetilde{K}_r^{\mathrm{on}}} + \frac{[\mathrm{BP}]}{\widetilde{K}_r^{\mathrm{on}}} \left(\frac{[\mathrm{L}]}{[\mathrm{L}]+K_{BP}} \right)}. \tag{8}$$

Alternatively, within Approximation 2, only the off receptor binds BP, giving

$$f_r = \epsilon_r + \log \left[1 + \frac{[\mathrm{BP_{closed}}]}{K_r^{\mathrm{off-closed}}} + \frac{[\mathrm{BP_{open}}]}{K_r^{\mathrm{off-open}}} \right], \tag{9}$$

which can we rewritten as

$$f_r = \epsilon_r + \log \left[1 + \frac{[\mathrm{BP}]}{\widetilde{K}_r^{\mathrm{open}}} + \frac{[\mathrm{BP}]}{\widetilde{K}_r^{\mathrm{closed}}} \left(\frac{[\mathrm{L}]}{[\mathrm{L}] + K_{BP}} \right) \right], \tag{10}$$

using the new parameters $\widetilde{K}_r^{\mathrm{closed}} = \left[(p_\infty - p_0)/K_r^{\mathrm{off-closed}} - (p_\infty - p_0)/K_r^{\mathrm{on-open}} \right]^{-1}$ and $\widetilde{K}_r^{\mathrm{open}} = \left[p_0/K_r^{\mathrm{off-closed}} + (1 - p_0)/K_r^{\mathrm{off-open}} \right]^{-1}$.

Approximation 2 is functionally identical to Approximation 1 in the limit of $[\mathrm{BP}] << \widetilde{K}_r^{\mathrm{on}}$, with the identifications $\widetilde{K}_r^{\mathrm{off}} \leftrightarrow \widetilde{K}_r^{\mathrm{closed}}$ and $\widetilde{p}_0 \leftrightarrow \widetilde{K}_r^{\mathrm{closed}}/\widetilde{K}_r^{\mathrm{open}}$. In this limit, binding of closed BPs to off receptors in the absence of ligand within Approximation 1 acts in a similar manner to binding of open BPs to off receptors within Approximation 2. In both cases, high concentrations of BP favor inactive receptors even in the absence of ligand.

Activity collapse

Within our model, receptor activity is determined by the free-energy difference between receptor on and off states. If adaptation returns this free-energy difference to a fixed value, the response of activity to a change in ligand concentration depends only on the free-energy change. Therefore, experimental dose-response curves should collapse when plotted as a function of the free-energy change. For different receptor types, the free-energy change must be weighted by the receptor proportion to yield an average, $\langle \delta f \rangle = (n_r/N)\delta f_r$, where n_r is the number of the receptor type r in a team of N receptors.

For comparison to experiment, we calculated the change in f_r upon addition of more ligand δ[L] to cells adapted to ambient ligand concentration [L]. For major receptors, the change in free-energy of receptor r is

$$\delta f_r = \log\left[1 + \frac{\delta[\mathrm{L}]}{[\mathrm{L}] + K_r^{\mathrm{off}}}\right] - \log\left[1 + \frac{\delta[\mathrm{L}]}{[\mathrm{L}] + K_r^{\mathrm{on}}}\right]. \tag{11}$$

For BP-binding ligands, within Approximation 1, from Eq. 8,

$$\delta f_r = \log\left[\frac{1 + \frac{\widetilde{p}_0[\mathrm{BP}]}{\widetilde{K}_r^{\mathrm{off}}} + \frac{[\mathrm{BP}]}{\widetilde{K}_r^{\mathrm{off}}}\left(\frac{[\mathrm{L}]+\delta[\mathrm{L}]}{[\mathrm{L}]+\delta[\mathrm{L}]+K_{BP}}\right)}{1 + \frac{\widetilde{p}_0[\mathrm{BP}]}{\widetilde{K}_r^{\mathrm{on}}} + \frac{[\mathrm{BP}]}{\widetilde{K}_r^{\mathrm{on}}}\left(\frac{[\mathrm{L}]+\delta[\mathrm{L}]}{[\mathrm{L}]+\delta[\mathrm{L}]+K_{BP}}\right)}\right] - \log\left[\frac{1 + \frac{\widetilde{p}_0[\mathrm{BP}]}{\widetilde{K}_r^{\mathrm{off}}} + \frac{[\mathrm{BP}]}{\widetilde{K}_r^{\mathrm{off}}}\left(\frac{[\mathrm{L}]}{[\mathrm{L}]+K_{BP}}\right)}{1 + \frac{\widetilde{p}_0[\mathrm{BP}]}{\widetilde{K}_r^{\mathrm{on}}} + \frac{[\mathrm{BP}]}{\widetilde{K}_r^{\mathrm{on}}}\left(\frac{[\mathrm{L}]}{[\mathrm{L}]+K_{BP}}\right)}\right]. \tag{12}$$

The above expression for δf_r has 4 unknown parameters: $\widetilde{K}_r^{\mathrm{on}}/[\mathrm{BP}]$, $\widetilde{K}_r^{\mathrm{off}}/[\mathrm{BP}]$, K_{BP}, and $\widetilde{p}_0$. This is one less parameter than we started with, reducing the difficulty of fitting the data, but also meaning that there is freedom in choosing one parameter to yield an identical set of dose-response curves. Here, Eq. 12 is unchanged under the simultaneous transformation $\widetilde{K}_r^{\mathrm{off/on}} \to \widetilde{K}_r^{\mathrm{off/on}\prime}$ and $\widetilde{p}_0 \to \widetilde{p}_0'$ if $\widetilde{K}_r^{\mathrm{off/on}} + \widetilde{p}_0[\mathrm{BP}] = \widetilde{K}_r^{\mathrm{off/on}\prime} + \widetilde{p}_0'[\mathrm{BP}]$.

Similarly for Approximation 2, from Eq. 10,

$$\delta f_r = \log\left[\frac{1 + \frac{[\mathrm{BP}]}{\widetilde{K}_r^{\mathrm{open}}} + \frac{[\mathrm{BP}]}{\widetilde{K}_r^{\mathrm{closed}}}\left(\frac{[\mathrm{L}]+\delta[\mathrm{L}]}{[\mathrm{L}]+\delta[\mathrm{L}]+K_{BP}}\right)}{1 + \frac{[\mathrm{BP}]}{\widetilde{K}_r^{\mathrm{open}}} + \frac{[\mathrm{BP}]}{\widetilde{K}_r^{\mathrm{closed}}}\left(\frac{[\mathrm{L}]}{[\mathrm{L}]+K_{BP}}\right)}\right]. \tag{13}$$

Here, the expression for δf_r has 3 unknown parameters: $\widetilde{K}_r^{\mathrm{closed}}/[\mathrm{BP}]$, $\widetilde{K}_r^{\mathrm{open}}/[\mathrm{BP}]$, and K_{BP}. Also, Eq. 13 is unchanged under the simultaneous transformation $\widetilde{K}_r^{\mathrm{closed}} \to \widetilde{K}_r^{\mathrm{closed}\prime}$ and $\widetilde{K}_r^{\mathrm{open}} \to \widetilde{K}_r^{\mathrm{open}\prime}$ if $\widetilde{K}_r^{\mathrm{closed}} + (\widetilde{K}_r^{\mathrm{closed}}/\widetilde{K}_r^{\mathrm{open}})[\mathrm{BP}] = \widetilde{K}_r^{\mathrm{closed}\prime} + (\widetilde{K}_r^{\mathrm{closed}\prime}/\widetilde{K}_r^{\mathrm{open}\prime})[\mathrm{BP}]$.

Response sensitivity

To characterize the dynamic range of response to ligand, we define the response sensitivity S_R as the derivative of the activity with respect to $\log[\mathrm{L}]$. This is directly analogous to the experimental definition of S_R as $d\mathrm{FRET}/d\log[\mathrm{L}]$. In the case of precise adaptation to activity A_0 the response sensitivity can also be written as

$$S_R = -\frac{[\mathrm{L}]}{A}\frac{dA}{d[\mathrm{L}]} = n_r(1-A_0)\frac{df_r}{d\log[\mathrm{L}]}. \tag{14}$$

For major ligands, the derivative of the receptor free energy with respect to $\log[\mathrm{L}]$ is given by

$$\frac{df_r}{d\log[\mathrm{L}]} = \frac{[\mathrm{L}]}{[\mathrm{L}]+K_r^{\mathrm{off}}} - \frac{[\mathrm{L}]}{[\mathrm{L}]+K_r^{\mathrm{on}}}. \tag{15}$$

In this case, the fold dynamic range of sensitive response depends only on the ratio $K_r^{\mathrm{on}}/K_r^{\mathrm{off}}$, since $df_r/d\log[\mathrm{L}]$ is only sizeable for [L] between $\sim K_r^{\mathrm{off}}$ and $\sim K_r^{\mathrm{on}}$. The response sensitivity at the peak of the dynamic range is given by

$$S_R^P = n_r(1-A_0)\frac{K_r^{\mathrm{on}}-K_r^{\mathrm{off}}}{\left(\sqrt{K_r^{\mathrm{on}}}+\sqrt{K_r^{\mathrm{off}}}\right)^2}, \tag{16}$$

at $[\mathrm{L}]^P = \sqrt{K_r^{\mathrm{off}}K_r^{\mathrm{on}}}$.

For the case of ligands that are bound by BPs, in Approximation 1, the derivative of f_r in Eq. 14 is given by

$$\frac{df_r}{d\log[\mathrm{L}]} = \frac{df_r}{d\log[\mathrm{BP}_{\mathrm{closed}}]}\frac{d\log[\mathrm{BP}_{\mathrm{closed}}]}{d\log[\mathrm{L}]}. \tag{17}$$

Within the model, the fall-off of response sensitivity at high [L] can be due to either a small receptor dynamic range (a decrease in $df_r/d\log[\mathrm{BP}_{\mathrm{closed}}]$) or a small BP dynamic range (a decrease in $d\log[\mathrm{BP}_{\mathrm{closed}}]/d\log[\mathrm{L}]$). If the fall-off is due to a small BP dynamic range, then the concentration [L] at which the fall-off occurs is $\approx K_{BP}$, independent of [BP]. In contrast, if the fall-off of S_R is due to a small receptor dynamic range, then the fall-off concentration [L] depends inversely on [BP]. Explicitly, the derivative of f_r is

$$\frac{df_r}{d\log[\mathrm{L}]} = \frac{[\mathrm{L}]K_{BP}\left(\widetilde{K}_r^{\mathrm{on}}/[\mathrm{BP}]-\widetilde{K}_r^{\mathrm{off}}/[\mathrm{BP}]\right)}{\left[[\mathrm{L}]+(K_{BP}+[\mathrm{L}])(\widetilde{K}_r^{\mathrm{off}}/[\mathrm{BP}]+\widetilde{p}_0)\right]\left[[\mathrm{L}]+(K_{BP}+[\mathrm{L}])(\widetilde{K}_r^{\mathrm{on}}/[\mathrm{BP}]+\widetilde{p}_0)\right]}, \tag{18}$$

and the maximum response sensitivity occurs at

$$[\mathrm{L}]^P = K_{BP}\sqrt{\frac{\left(\widetilde{K}_r^{\mathrm{off}}/[\mathrm{BP}]+\widetilde{p}_0\right)\left(\widetilde{K}_r^{\mathrm{on}}/[\mathrm{BP}]+\widetilde{p}_0\right)}{\left(\widetilde{K}_r^{\mathrm{off}}/[\mathrm{BP}]+\widetilde{p}_0+1\right)\left(\widetilde{K}_r^{\mathrm{on}}/[\mathrm{BP}]+\widetilde{p}_0+1\right)}} \equiv \gamma K_{BP}. \tag{19}$$

The maximum sensitivity is independent of K_{BP} and given by

$$S_R^P = n_r(1-A_0)\frac{\gamma\left(\widetilde{K}_r^{\rm on}/[{\rm BP}]-\widetilde{K}_r^{\rm off}/[{\rm BP}]\right)}{\left[\gamma+(1+\gamma)\left(\widetilde{K}_r^{\rm off}/[{\rm BP}]+\widetilde{p}_0\right)\right]\left[\gamma+(1+\gamma)\left(\widetilde{K}_r^{\rm on}/[{\rm BP}]+\widetilde{p}_0\right)\right]}. \quad (20)$$

Here, in contrast to major receptors, maximum response sensitivity does not just depend on the ratio $\widetilde{K}_r^{\rm on}/\widetilde{K}_r^{\rm off}$, because the total binding protein concentration [BP] is also involved. S_R^P is a decreasing function of $\widetilde{p}_0$, and in the limit of a BP with an extremely stable open state, *i.e.* with $\widetilde{p}_0 = 0$, S_R^P increases with [BP] to reach the maximum limit of

$$S_R^{P,{\rm limit}} = n_r(1-A_0)\frac{\widetilde{K}_r^{\rm on}-\widetilde{K}_r^{\rm off}}{\left(\sqrt{\widetilde{K}_r^{\rm on}}+\sqrt{\widetilde{K}_r^{\rm off}}\right)^2}. \quad (21)$$

However, if $\widetilde{p}_0 > 0$, then S_R^P has a maximum at a specific [BP] and decreases to zero at high [BP]. The decrease in sensitivity at high [BP] occurs because, even in the absence of ligand, there are enough closed BPs to saturate the receptors. For a particular value of $\widetilde{p}_0$, this loss of sensitivity due to receptor saturation occurs at [BP] $\approx \widetilde{K}_r^{\rm on}/\widetilde{p}_0$.

Within the model, we can easily separate decreases in response sensitivity due to a small dynamic range of the receptor-BP interaction (21) from "inefficiency" of the BP (20). The BP can be inefficient due to having too large a value of $\widetilde{p}_0$ and/or not having a maximally efficient BP concentration. The decrease in sensitivity due to the dynamic range of the receptor is determined by the ratio of the peak response sensitivity S_R^P to the limit of S_R^P as $\widetilde{K}_r^{\rm on} \to \infty$. This ratio will approach 1 for a receptor that has a large dynamic range. The inefficiency of the BP can be gauged by the ratio $S_R^P/S_R^{P,{\rm limit}}$, which will approach 1 for a maximally efficient BP, *i.e.* one with $\widetilde{p}_0 \approx 0$, provided [BP] $> \widetilde{K}_r^{\rm on}$.

The results simplify if $\widetilde{K}_r^{\rm off} << [{\rm BP}] << \widetilde{K}_r^{\rm on}$ and $\widetilde{p}_0 << 1$, to

$$[{\rm L}]^P \approx K_{BP}\sqrt{\widetilde{K}_r^{\rm off}/[{\rm BP}]+\widetilde{p}_0}, \quad (22)$$

and

$$S_R^P \approx n_r(1-A_0)\left[1-2\sqrt{\widetilde{K}_r^{\rm off}/[{\rm BP}]+\widetilde{p}_0}\right], \quad (23)$$

the approximations used in the main text.

Within Approximation 2,

$$\frac{df_r}{d\log[{\rm L}]} = \frac{[{\rm L}]K_{BP}}{([{\rm L}]+K_{BP})\left[[{\rm L}]+(K_{BP}+[{\rm L}])\left(\widetilde{K}_r^{\rm closed}/[{\rm BP}]+\widetilde{K}_r^{\rm closed}/\widetilde{K}_r^{\rm open}\right)\right]}, \quad (24)$$

where only 1 parameter, $\widetilde{K}_r^{\rm closed}/[{\rm BP}] + \widetilde{K}_r^{\rm closed}/\widetilde{K}_r^{\rm open}$, controls the sensitivity at the level of the receptor-BP interaction. The maximum sensitivity occurs at

$$[{\rm L}]^P = K_{BP}\sqrt{\frac{\widetilde{K}_r^{\rm closed}/[{\rm BP}] + \widetilde{K}_r^{\rm closed}/\widetilde{K}_r^{\rm open}}{1+\widetilde{K_r}^{\rm closed}/[{\rm BP}] + \widetilde{K}_r^{\rm closed}/\widetilde{K}_r^{\rm open}}}, \tag{25}$$

and the maximum sensitivity is given by

$$\begin{aligned} S_R^P = n_r(1-A_0)\Big[1 + 2\left(\widetilde{K}_r^{\rm closed}/[{\rm BP}] + \widetilde{K}_r^{\rm closed}/\widetilde{K}_r^{\rm open}\right) \\ - 2\sqrt{\widetilde{K}_r^{\rm closed}/[{\rm BP}] + \widetilde{K}_r^{\rm closed}/\widetilde{K}_r^{\rm open}}\sqrt{1+\widetilde{K}_r^{\rm closed}/[{\rm BP}] + \widetilde{K}_r^{\rm closed}/\widetilde{K}_r^{\rm open}}\Big]. \end{aligned} \tag{26}$$

Here, maximum sensitivity increases with [BP] to reach the maximum limit of

$$S_R^{P,{\rm limit}} = n_r(1-A_0)\left[1 + 2\widetilde{K}_r^{\rm closed}/\widetilde{K}_r^{\rm open} - 2\sqrt{\widetilde{K}_r^{\rm closed}/\widetilde{K}_r^{\rm open}}\sqrt{1+\widetilde{K}_r^{\rm closed}/\widetilde{K}_r^{\rm open}}\right]. \tag{27}$$

As in Approximation 1, we can separate a decrease in response sensitivity due to the receptor binding BP in the absence of ligand (27) from a decrease due to an inefficient BP concentration (26). The decrease in sensitivity due to receptor binding of BPs in the absence of ligand is determined by the ratio of the peak response S_R^P to the value of S_R^P in the limit of $\widetilde{K}_r^{\rm open} \to \infty$. The inefficiency of the BP concentration can then be gauged by the ratio $S_R^P/S_R^{P,{\rm limit}}$, which will approach 1 for a large BP concentration.

The results simplify in the limit $\widetilde{K}_r^{\rm open} >> \widetilde{K}_r^{\rm closed}$, $[{\rm BP}] >> \widetilde{K}_r^{\rm closed}$, yielding

$$[{\rm L}]^P \approx K_{BP}\sqrt{\widetilde{K}_r^{\rm closed}/[{\rm BP}] + \widetilde{K}_r^{\rm closed}/\widetilde{K}_r^{\rm open}}, \tag{28}$$

and

$$S_R^P \approx n_r(1-A_0)\left[1 - 2\sqrt{\widetilde{K}_r^{\rm closed}/[{\rm BP}] + \widetilde{K}_r^{\rm closed}/\widetilde{K}_r^{\rm open}}\right]. \tag{29}$$

Threshold sensitivity

Here we calculate the threshold sensitivity S_T, which is the inverse of the ligand concentration that yields of half-maximal activity. To reach half-maximal activity, $A_0/2$, according to Eq. 1 the free-energy change must be

$$\delta f_r = \frac{1}{n_r}\log\left(\frac{2-A_0}{1-A_0}\right). \tag{30}$$

For receptors that directly bind ligand, starting at zero ambient ligand and setting $\delta \mathrm{L} = [\mathrm{L}]_{1/2}$ in Eq. 11, the theshold sensitivity $S_T = 1/[\mathrm{L}]_{1/2}$ is

$$S_T = \frac{\frac{1}{K_r^{\mathrm{off}}} - \frac{1}{K_r^{\mathrm{on}}} \left(\frac{2-A_0}{1-A_0}\right)^{1/n_r}}{\left(\frac{2-A_0}{1-A_0}\right)^{1/n_r} - 1}. \tag{31}$$

Therefore, for $K_r^{\mathrm{off}} << K_r^{\mathrm{on}}$ and $n_r >> 1$, one finds

$$S_T \approx n_r \frac{1}{K_r^{\mathrm{off}}} \left[\log\left(\frac{2-A_0}{1-A_0}\right)\right]^{-1}. \tag{32}$$

For BP-binding ligands, in Approximation 1, starting at zero ambient ligand and setting $\delta \mathrm{L} = [\mathrm{L}]_{1/2}$, the change in free energy from Eq. 12 reduces to

$$\delta f_r = \log \frac{1 + \frac{1}{\widetilde{K}_r^{\mathrm{off}}/[\mathrm{BP}]+\widetilde{p}_0} \left(\frac{[\mathrm{L}]_{1/2}}{[\mathrm{L}]_{1/2}+K_{BP}}\right)}{1 + \frac{1}{\widetilde{K}_r^{\mathrm{on}}/[\mathrm{BP}]+\widetilde{p}_0} \left(\frac{[\mathrm{L}]_{1/2}}{[\mathrm{L}]_{1/2}+K_{BP}}\right)}. \tag{33}$$

Solving for $S_T = 1/[\mathrm{L}]_{1/2}$ yields

$$S_T = \frac{1}{K_{BP}} \frac{\left(1 + \frac{1}{\widetilde{K}_r^{\mathrm{off}}/[\mathrm{BP}]+\widetilde{p}_0}\right) - \left(\frac{2-A_0}{1-A_0}\right)^{1/n_r} \left(1 + \frac{1}{\widetilde{K}_r^{\mathrm{on}}/[\mathrm{BP}]+\widetilde{p}_0}\right)}{\left(\frac{2-A_0}{1-A_0}\right)^{1/n_r} - 1}. \tag{34}$$

As with S_R^P, S_T reaches has a maximum with respect to [BP], and decreases above $[\mathrm{BP}] \approx \widetilde{K}_r^{\mathrm{on}}/\widetilde{p}_0$ as receptors become saturated with BP in the absence of ligand. If $[\mathrm{BP}] << \widetilde{K}_r^{\mathrm{off}}/\widetilde{p}_0$, *i.e.* receptors do not strongly bind BP in the absence of ligand, then S_T increases linearly with [BP] as

$$S_T \approx \frac{1}{K_{BP}} \frac{[\mathrm{BP}] \left[\frac{1}{\widetilde{K}_r^{\mathrm{off}}} + \frac{1}{\widetilde{K}_r^{\mathrm{on}}} \left(\frac{2-A_0}{1-A_0}\right)^{1/n_r}\right] + \left[1 - \left(\frac{2-A_0}{1-A_0}\right)^{1/n_r}\right]}{\left(\frac{2-A_0}{1-A_0}\right)^{1/n_r} - 1}. \tag{35}$$

Under the different limit $[\mathrm{BP}] << \widetilde{K}_r^{\mathrm{on}}$ and $\widetilde{p}_0 << 1$, then

$$S_T \approx \frac{1}{K_{BP}} \frac{1}{\widetilde{p}_0} \left[\left(\frac{2-A_0}{1-A_0}\right)^{1/n_r} - 1\right]^{-1} \frac{[\mathrm{BP}]}{[\mathrm{BP}] + \widetilde{K}_r^{\mathrm{off}}/\widetilde{p}_0}, \tag{36}$$

which has simple hyperbolic dependence on [BP] for all n_r and A_0. Also for $n_r >> 1$, S_T given by Eq. 36 increases approximately linearly with n_r as

$$S_T \approx n_r \frac{1}{K_{BP}} \frac{1}{\widetilde{p}_0} \left[\log\left(\frac{2-A_0}{1-A_0}\right)\right]^{-1} \frac{[\mathrm{BP}]}{[\mathrm{BP}] + \widetilde{K}_r^{\mathrm{off}}/\widetilde{p}_0}, \tag{37}$$

which is the approximation used in the main text.

Within Approximation 2, from Eq. 13,

$$\delta f_r = \log\left[\frac{1+\frac{[\mathrm{BP}]}{\widetilde{K}_r^{\mathrm{open}}}+\frac{[\mathrm{BP}]}{\widetilde{K}_r^{\mathrm{closed}}}\left(\frac{[\mathrm{L}]_{1/2}}{[\mathrm{L}]_{1/2}+K_{BP}}\right)}{1+\frac{[\mathrm{BP}]}{\widetilde{K}_r^{\mathrm{open}}}}\right], \tag{38}$$

and

$$S_T = \frac{1}{K_{BP}}\left(\frac{\widetilde{K}_r^{\mathrm{open}}}{\widetilde{K}_r^{\mathrm{closed}}\left(1+\widetilde{K}_r^{\mathrm{open}}/[\mathrm{BP}]\right)}\left[\left(\frac{2-A_0}{1-A_0}\right)^{1/n_r}-1\right]^{-1}-1\right). \tag{39}$$

Here, S_T saturates with increasing [BP] above $[\mathrm{BP}] > \widetilde{K}_r^{\mathrm{open}}$ as receptor begin to significantly bind open BP. If $\widetilde{K}_r^{\mathrm{open}} >> \widetilde{K}_r^{\mathrm{closed}}$, then this expression reduces to

$$S_T \approx \frac{1}{K_{BP}}\frac{\widetilde{K}_r^{\mathrm{open}}}{\widetilde{K}_r^{\mathrm{closed}}}\left[\left(\frac{2-A_0}{1-A_0}\right)^{1/n_r}-1\right]^{-1}\frac{[\mathrm{BP}]}{[\mathrm{BP}]+\widetilde{K}_r^{\mathrm{open}}}, \tag{40}$$

which like Eq. 37 also has simple hyperbolic dependence on [BP] for all n_r and A_0. Similarly, for $n_r >> 1$, S_T in Eq. 40 increases approximately linearly with n_r as

$$S_T \approx n_r\frac{1}{K_{BP}}\frac{\widetilde{K}_r^{\mathrm{open}}}{\widetilde{K}_r^{\mathrm{closed}}}\left[\log\left(\frac{2-A_0}{1-A_0}\right)\right]^{-1}\frac{[\mathrm{BP}]}{[\mathrm{BP}]+\widetilde{K}_r^{\mathrm{open}}}. \tag{41}$$

Results of activity collapse

Figure 5 in the main text shows the activity collapse for WT cells using Approximation 1 and Fig. A shows the activity collapse using Approximation 2. We did not include the dynamic range responses at high concentrations of Galactose, Maltose, and Ribose, which are due to sugar taxis. We also did not include Serine in the collapse because there is an additional unknown sensory mechanism (Fig. S6). In estimating the receptor proportions, we did not include Aer because it is a small fraction of the total receptor pool and does not bind any of the ligands considered. Including Aer would decrease the average free-energy change per receptor, shifting the free-energy collapse slightly to the left.

Figure B shows the collapse for Galactose at different BP induction levels using Approximation 1. The binding parameters (Table A) for each ligand were determined through the use of dose-response and dynamic-range measurements for both WT (LJ110) cells and

also cells at different BP induction levels. The activity collapses using Approximation 1 and Approximation 2 are very similar in quality, even though Approximation 1 includes an additional free parameter compared to Approximation 2. Within Approximation 1, the collapses are very similar for a wide range of the parameters $\widetilde{K}_r^{\rm on}$ and $\widetilde{p}_0$ as lower $\widetilde{K}_r^{\rm on}$ and higher $\widetilde{p}_0$ both decrease the sensitivity to ligand, and therefore can interchange to a degree. If $\widetilde{p}_0$ is too low, though, lower $\widetilde{K}_r^{\rm on}$ cannot substitute for a good fit since a low $\widetilde{p}_0$ predicts that S_T increases linearly with [BP]. Instead, a higher $\widetilde{p}_0$ predicts that S_T saturates with increasing [BP], as is experimentally observed. On the other hand, if $\widetilde{p}_0$ is chosen too high, the sensitivity decreases below the observed values even in the limit of $\widetilde{K}_r^{\rm on} >> [\mathrm{BP}]$.

As explained in the section *Free-energy model for receptor teams*, Approximation 1 in the limit of $\widetilde{K}_r^{\rm on} \to \infty$ is functionally identical to Approximation 2, as finite $\widetilde{p}_0$ in Approximation 1 allows closed BP-receptor binding in the absence of ligand, playing a similar role to open BP-receptor binding in Approximation 2. Therefore, since sensitivity decreases due to nonzero $\widetilde{p}_0$ or finite $\widetilde{K}_r^{\rm on}$ can trade off to a degree over a large range, we found that including BP binding to on receptors does not significantly improve the activity collapse. This is true unless S_T or S_R^P begin to decrease at high levels of [BP], which would indicate BP binding to on receptors. This decrease of sensitivity at high [BP] is is not experimentally observed. Instead, both S_R and S_T seem to saturate at high levels of [BP], but because higher levels of [BP] were not analyzed, we are not certain whether S_R or S_T would decrease at even higher levels of [BP].

Fits for both Approximation 1 and 2 (see Table A) indicate that S_R is much lower than the maximum possible value of 1. For major ligands, loss of response sensitivity is due to binding of ligand by on receptors, but for BP-binding receptors in addition to binding of closed BP by on receptors, additional losses in sensitivity may occur because: (i) receptors bind to open BPs, (ii) there are some closed BPs even in the absence of ligand, and (iii) the BP concentration may be nonoptimal. These additional factors help explain the lower sensitivies observed for receptors that bind BPs compared to receptors that bind ligand directly.

While both Approximations fit the FRET data well, they differ in the proportion of BP-bound receptors in the absence of ligand. For adapting cells with activity A_0, the proportion of BP-bound receptors in the absence of ligand is $\approx(1-A_0)[\mathrm{BP}]/(\widetilde{K}_r^{\rm off}/\widetilde{p}_0+[\mathrm{BP}])$, while within Approximation 2, the proportion is $\approx(1-A_0)[\mathrm{BP}]/(\widetilde{K}_r^{\rm open}+[\mathrm{BP}])$, in both cases

simply reflecting the equilibrium binding of BP to off receptors. Within Approximation 1, we were able to find lower values of $\widetilde{p}_0$ within the range of adequately similar activity collapses, consistent with a low proportion of occupied receptors. From the fitted parameter values (Table A), the proportion of bound receptors in the absence of ligand is larger in Approximation 2 than Approximation 1. Since higher levels of occupied receptors will decrease sensitivity to other BPs or ligands that bind the same receptor type, we have presented Approximation 1 in the main text because we believe it is more likely to capture the true parameter regime.

---

[1] Mello B A, Tu Y (2005) An allosteric model for heterogeneous receptor complexes: Understanding bacterial chemotaxis responses to multiple stimuli Proc Natl Acad Sci USA 102: 17354-17359.

[2] Keymer JE, Endres RG, Skoge M, Meir Y, Wingreen NS (2006) Chemosensing in *Escherichia coli*: two regimes of two-state receptors. Proc Natl Acad Sci USA 103: 1786-1791.

[3] Endres RG, Wingreen NS (2006) Precise adaptation in bacterial chemotaxis through 'assistance neighborhoods'. Proc Natl Acad Sci USA, 103: 13040-13044.

[4] Hansen CH, Endres RG, Wingreen NS (2008) Chemotaxis in Escherichia coli: a molecular model for robust precise adaptation. PLoS Comput Biol 4, e1.

(1)

	$K_{BP}(\mu\mathrm{M})$	$\widetilde{K}_r^{\mathrm{off}}/[\mathrm{BP}]$	$\widetilde{K}_r^{\mathrm{on}}/[\mathrm{BP}]$	$\widetilde{p}_0$
Galactose	0.3	0.07	0.7	0.1
Dipeptide	2	0.4	1.3	0.1
Ribose	1	0.1	6	0.1
Maltose	2	0.4	6	0.1

(2)

	$K_{BP}(\mathrm{mM})$	$\widetilde{K}_r^{\mathrm{closed}}/[\mathrm{BP}]$	$\widetilde{K}_r^{\mathrm{open}}/[\mathrm{BP}]$
Galactose	0.15	0.08	0.2
Dipeptide	1	0.7	0.8
Ribose	0.8	0.1	0.7
Maltose	1.5	0.5	2

Table A. Fitted parameters for ligands that bind BPs. The free-energy model is described in the SI and results are shown for both (1) Approximation 1 and (2) Approximation 2. Parameters were obtained through activity collapse of normalized dose-response and dynamic range curves of both wild-type cells and cells at different BP induction levels. For MeAsp binding to Tar: $K_{\mathrm{tar}}^{\mathrm{off}} = 30\,\mu\mathrm{M}$ and $K_{\mathrm{tar}}^{\mathrm{on}} = 500\,\mu\mathrm{M}$, for Asp binding to Tar: $K_{\mathrm{tar}}^{\mathrm{off}} = 1.5\,\mu\mathrm{M}$ and $K_{\mathrm{tar}}^{\mathrm{on}} = 20\,\mu\mathrm{M}$, for Asp binding to Tsr: $K_{\mathrm{tar}}^{\mathrm{off}} = 10^5\,\mu\mathrm{M}$, and for AiBu binding to Tsr: $K_{\mathrm{tsr}}^{\mathrm{off}} = 500\,\mu\mathrm{M}$ and $K_{\mathrm{tsr}}^{\mathrm{on}} = 3000\,\mu\mathrm{M}$.

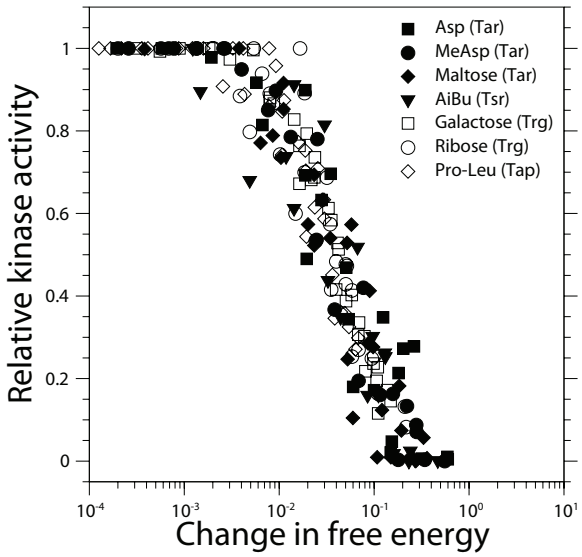

Figure A. Collapse of receptor activity when plotted as a function of free energy using Approximation 2. Results are shown for wild-type cells responding to the ligands MeAsp, AiBu, Galactose, Dipeptide, Ribose, and Maltose. Binding parameters were obtained through the collapse of normalized dose-response and dynamic-range curves of both wild-type cells and cells at different BP induction levels. The free-energy model for BP-binding ligands is described in the SI and binding parameters are given in SI Table A2.

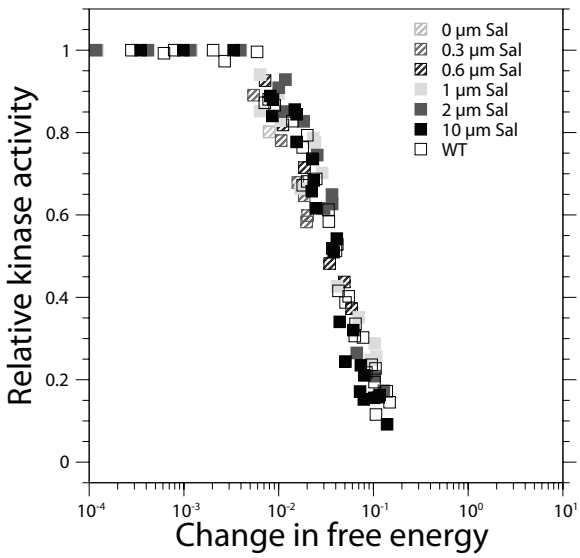

Figure B. Collapse of receptor activity when plotted as a function of free energy under stimulation by Galactose, using Approximation 1. Results are shown for normalized dose-response and dynamic-range curves of both wild-type cells and cells at different BP induction levels. For different BP induction levels, the galactose BP MglB was expressed from plasmid pSN76 in strain SN28. Expression of MglB was estimated to be proportional to the expression of YFP under the same promoter, measured as described in SI Materials and Methods. Binding parameters are the same as in Fig. 5 and are given in SI Table A1.